



UNIVERSITAT  
POLITÈCNICA  
DE VALÈNCIA

**UNIVERSITAT POLITÈCNICA DE VALÈNCIA**

ESCUELA TÉCNICA SUPERIOR DE INGENIERÍA DEL DISEÑO

**TRABAJO FIN DE MÁSTER**

Máster Universitario en Ingeniería Aeronáutica

**PARAMETRIC STUDY OF AN UNMIXED FLOW  
TURBOFAN ENGINE FOR PERFORMANCE  
IMPROVEMENT UNDER DESIGN CONDITIONS**

Autor del trabajo  
**Álvaro Vega Asensio**

Tutor del trabajo  
**Sergio Hoyas Calvo**

Julio de 2019



# Acknowledgements

Vorrei innanzitutto ringraziare l'Università degli Studi "La Sapienza", a Roma, per l'opportunità che mi hanno dato permettendomi di studiare l'ultimo anno della mia carriera all'estero, che mi ha arricchito sia come studente che come persona.

Ringrazio il Dipartimento di Ingegneria Meccanica e Aerospaziale, e in particolare il professor Mauro Valorani, per la fiducia che hanno riposto in me per la realizzazione di questo progetto. Grazie Professore per avermi protetto e per avermi guidato nella realizzazione di questo lavoro.

Ringrazio anche Riccardo e Pietro per il loro aiuto in questi mesi e per la loro completa disponibilità ogni volta che sono andato a consultarli per dubbi o proposte per il progetto.

Anche, vorrei ringraziare al personale di ESTECO, in particolare alla signora Sara Bortolozzo, per avermi gentilmente procurato la licenza del software ModeFrontier<sup>®</sup> durante tutto il tempo di sviluppo del progetto.

Finalmente, me gustaría agradecer al profesor Sergio Hoyas, de la Universitat Politècnica de València, por haber aceptado ser mi tutor en la susodicha Universidad.



## RESUMEN

Desde que la aviación comenzara su andadura a comienzos del siglo XX, el desarrollo de una planta propulsora ha sido siempre clave en la evolución de esta disciplina: desde los primeros motores de combustión interna alternativos hasta los más modernos turbofan de flujo mezclado, en todos ellos se ha buscado la mejora de las prestaciones con la más adecuada gestión de los recursos posible. Hoy en día, y en el ámbito de la aviación comercial, dicha optimización versa sobre la reducción del consumo del motor, a la vez que se garantiza el empuje requerido por la aeronave.

El trabajo llevado a cabo en el presente documento tiene como objetivo la mejora y optimización de las prestaciones de un motor de tipo turbofan de flujo separado en fase de crucero. Se seleccionarán los parámetros característicos del motor que modificar para encontrar el óptimo y se buscará una solución satisfactoria en términos de empuje y consumo específico, al mismo tiempo que se intentará reducir la relación peso-empuje del conjunto. Para el cálculo de prestaciones, se ha modelado analíticamente el ciclo termodinámico que envuelve al motor, mientras que para su optimización se ha empleado *software* especializado en el tema. Dicho estudio permitirá conocer las características del motor que idealmente permite volar de la manera más eficiente posible.

Este proyecto se ha desarrollado con la ayuda de Wolfram Mathematica<sup>®</sup> y ModeFrontier<sup>®</sup>, mediante la creación de librerías que permite obtener de manera sencilla las prestaciones del motor cuyos parámetros de diseño son introducidos por el usuario.

Finalmente, se procede a validar y discutir los resultados obtenidos, aplicando literatura específica del tema y estudiando las variables que influyen en el fenómeno, con el fin de proporcionar unos resultados veraces y con aplicabilidad en el sector.



## ABSTRACT

Since aviation began at the beginning of the 20th century, the development of a propulsion plant has always been a key factor in the evolution of this discipline: from the first internal combustion engines to the most modern mixed flow turbofans, all of them have sought to improve performance with the most appropriate management of resources possible. Today, in the field of commercial aviation, this optimisation concerns the reduction of engine consumption, guaranteeing at the same time the thrust required by the aircraft.

The work carried out in this document aims to improve and optimise the performance of a separate flow turbofan engine during the cruising phase. Engine characteristic parameters to be modified for the optimum search will be selected, and a trade-off between thrust specific fuel consumption and specific thrust will be found, attempting at the same time a reduction in the weight-to-thrust ratio of the whole. For performance calculation, the thermodynamic cycle surrounding the engine has been analytically modeled, whereas specialised software has been used to optimise it. This study will allow the knowledge of the characteristics of the engine that ideally allow to fly in the most efficient way.

This project has been developed with the help of Wolfram Mathematica<sup>®</sup> and ModeFrontier<sup>®</sup>, through the creation of libraries that allow to obtain in a simple way the engine features whose design parameters are introduced by the user.

Finally, validation and discussion of the results are conducted, applying specific literature on the subject and studying the variables that influence the phenomenon, in order to provide truthful results with applicability in the sector.





## ASTRATTO

Dall'inizio dell'aviazione all'inizio del XX secolo, lo sviluppo di un impianto di propulsione è sempre stato un fattore chiave nell'evoluzione di questa disciplina: dai primi motori a combustione interna alternativi ai più moderni turboventole a flusso misto, tutti hanno cercato di migliorare le prestazioni con la più appropriata gestione delle risorse possibili. Oggi, nel campo dell'aviazione commerciale, questa ottimizzazione riguarda la riduzione dei consumi del motore, garantendo al tempo stesso la spinta richiesta dal velivolo.

Il lavoro svolto in questo documento ha lo scopo di migliorare e ottimizzare le prestazioni di un motore a turboventola a flusso separato durante la fase di crociera. Verranno selezionati i parametri caratteristici del motore da modificare per trovare quello ottimale, e si cercherà una soluzione soddisfacente in termini di spinta e consumo specifico, cercando allo stesso tempo di ridurre il rapporto peso-spinta dell'insieme. Per il calcolo delle prestazioni, il ciclo termodinamico che circonda il motore è stato modellato analiticamente, mentre per ottimizzarlo è stato utilizzato un software specializzato. Questo studio permetterà di conoscere le caratteristiche del motore che idealmente permette di volare nel modo più efficiente possibile.

Questo progetto è stato sviluppato con l'aiuto di Wolfram Mathematica<sup>®</sup> e ModeFrontier<sup>®</sup>, attraverso la creazione di librerie che permettono di ottenere in modo semplice le caratteristiche del motore i cui parametri di progetto vengono introdotti dall'utente.

Infine, si procede alla validazione e discussione dei risultati ottenuti, applicando una letteratura specifica sull'argomento e studiando le variabili che influenzano il fenomeno, al fine di fornire risultati veritieri e applicabili nel settore.



# Keywords

Turbofan, unmixed flow, parametric study, design conditions



# Nomenclature

## Latin

$A$	—	Nozzle cross area
$C_1$	—	Torenbeek's correlation coefficient
$C_2$	—	Torenbeek's correlation coefficient
$c_p$	—	Pressure heat capacity
$D$	—	Drag
$f$	—	Fuel to air ratio
$FN$	—	Specific thrust
$g$	—	Earth gravity
$h, \Delta h$	—	Entalpy
$L, Q$	—	Heat of combustion
$M$	—	Mach number
$\dot{m}$	—	Massflow
$p$	—	Pressure
$R^2$	—	Pearson correlation coefficient
$T$	—	Temperature
	—	Thrust
$V$	—	Velocity
$z$	—	Altitude

## Greek

$\beta$	—	Bypass ratio
	—	Pressure ratio
$\gamma$	—	Heat capacity ratio
$\eta$	—	Efficiency
	—	Isentropic efficiency
$\rho$	—	Density

## Subscripts

0	—	Farfield
	—	Air
	—	Sea level conditions
11	—	At 11000 <i>m</i> , altitude
19	—	Secondary nozzle exhaust

2	—	Difusor exit
21	—	Fan exit
3	—	Compressor exit
4	—	Combustion chamber exit
41	—	High pressure turbine exit
5	—	Fan turbine exit
6	—	Afterburner exit
9	—	Primary nozzle exit
<i>a, air</i>	—	Air
<i>ad</i>	—	Additional
<i>b</i>	—	Burner
<i>c</i>	—	Compressor
	—	Combustion chamber
<i>d</i>	—	Difussor
<i>ext</i>	—	External
<i>f</i>	—	Fuel
<i>gas</i>	—	Air-fuel mix
<i>gg</i>	—	Gas generator
<i>ins</i>	—	Internal
<i>loss</i>	—	Loss
<i>m</i>	—	Mechanical
<i>n</i>	—	Nozzle
<i>p</i>	—	Pressure
<i>s</i>	—	Isentropic process
<i>t</i>	—	Stagnation
	—	Turbine
<i>th</i>	—	Thermal
	—	Theoretical
$\pi$	—	Primary flow
$\sigma$	—	Secondary flow

## Superscripts

*	—	Critical conditions
---	---	---------------------

## Acronyms

<i>BPR</i>	—	Bypass ratio
<i>NO<sub>x</sub></i>	—	Nitrogen oxides
<i>OPR</i>	—	Overall pressure ratio
<i>TIT</i>	—	Turbine inlet temperature
<i>TS</i>	—	Specific thrust
<i>TSFC</i>	—	Thrust specific fuel consumption
<i>WT, WTT</i>	—	Weight-to-thrust ratio

# Contents

1	Introduction . . . . .	1
1.1	Incentive, justification and objectives . . . . .	1
1.1.1	Justification . . . . .	1
1.1.2	Incentive . . . . .	1
1.1.3	Objectives . . . . .	1
2	Theoretical background . . . . .	3
2.1	Introduction . . . . .	3
2.2	Gas turbine engines . . . . .	3
2.2.1	Clasification . . . . .	3
2.2.2	The turbofan engine . . . . .	5
2.2.3	Range of usage . . . . .	6
2.3	The Brayton cycle in a turbofan . . . . .	8
2.3.1	Preliminary hypothesis . . . . .	9
2.3.2	Intake . . . . .	10
2.3.3	Fan . . . . .	11
2.3.4	Compressor . . . . .	12
2.3.5	Combustion chamber . . . . .	13
2.3.6	Turbine . . . . .	14
2.3.7	Afterburner . . . . .	16
2.3.8	Nozzle . . . . .	17
2.3.9	Bypassed flow . . . . .	19
2.4	Engine performance . . . . .	20
2.4.1	Specific thrust . . . . .	20
2.4.2	Specific consumption . . . . .	21
2.4.3	Specific impulse . . . . .	21
2.4.4	Thermal efficiency . . . . .	21
2.4.5	Propulsive efficiency . . . . .	22
2.4.6	Global efficiency . . . . .	22
2.4.7	Parameters interaction . . . . .	23
2.4.8	Engine weight . . . . .	23
3	Methodology . . . . .	25
3.1	Introduction . . . . .	25
3.2	Engine performance estimation . . . . .	25
3.2.1	Required information . . . . .	25
3.2.2	Implemented code . . . . .	27
3.3	Optimization procedure . . . . .	31
3.3.1	Working frame . . . . .	31
3.3.2	Design of experiments . . . . .	33
3.3.3	Sensitivity analysis . . . . .	34

	3.3.4	Optimization algorithm configuration . . . . .	37
4		Results . . . . .	41
	4.1	Sensitivity between input and output variables . . . . .	41
	4.2	Selection of the optimum . . . . .	43
	4.2.1	Summary and comparision of solutions presented . . . . .	46
	4.3	Influence of other parameters . . . . .	48
	4.3.1	Mission parameters . . . . .	48
	4.3.2	Component efficiencies . . . . .	55
5		Discussion of results . . . . .	61
6		Conclusions and future works . . . . .	63
	6.1	Conclusions . . . . .	63
	6.2	Future works . . . . .	63



# List of Figures

2.1	Draw of reaction engines classification.	4
2.2	Diagram of a two-spool unmixed flow turbofan engine. Source:[1]	5
2.3	Turbofan engines classification, attending to different criteria. Source:[2]	6
2.4	Aerospace jet engines applicability based on flight velocity and specific impulse. Specific impulse can be modeled, as a first approach, as the inverse of the specific fuel consumption. Source: [3].	7
2.5	Aerospace jet engines applicability based on flight velocity and specific fuel consumption. Source: [4]	7
2.6	Brayton cycle in a turbofan engine.	9
2.7	Detail of the intake part in the Brayton cycle.	11
2.8	Detail of the fan part in the Brayton cycle.	11
2.9	Detail of the compression part in the Brayton cycle.	13
2.10	Detail of the combustion in the Brayton cycle.	14
2.11	Detail of the high pressure turbine in the Brayton cycle.	16
2.12	Detail of the fan turbine in the Brayton cycle.	16
2.13	Detail of the primary nozzle in the Brayton cycle.	18
2.14	Detail of the secondary nozzle in the Brayton cycle.	20
3.1	Example of a <i>design_parameters.txt</i> file.	27
3.2	From left to right and top to bottom: air temperature, pressure and density according to ISA model.	29
3.3	Relative error between real engine weight and correlations studied for according to BPR.	30
3.4	Example of a <i>results.txt</i> file.	31
3.5	Workflow used for the study of the optimum design point.	32
3.6	Example of a 2D (left) and 3D (right) full factorial DOE.	34
3.7	Example of a 2D (left) and 3D (right) sobol DOE.	34
3.8	Example of linear relations between variables. Correlation matrix is plotted in the lower left corner and the scatter matrix can be found in the upper right one.	35
3.9	Example of pie chart based on a t-Student analysis.	36
3.10	Example of a parallel coordinates chart.	36
3.11	Example of a sensitivity chart.	37
3.12	MOGA-II workflow.	38
4.1	Correlation matrix involving design and performance parameters.	41
4.2	Scatter plot between bypass ratio and fuel consumption. TSFC is represented in SI units.	42
4.3	Overall t-student analysis of the study conducted.	43
4.4	Engine performance according to design parameters stated and optimization algorithm used. All units correspond to SI.	44
4.5	Pareto front of the engine performance. All units correspond to SI.	44

4.6	Solutions presented in the bubble chart (left) and together with whole Pareto front (right).	46
4.7	Brayton cycle comparing a low (black) and high (red) OPR engine.	47
4.8	From left to right and top to bottom: engine performance variation as a function of mission parameters for configuration solution D.	49
4.9	From left to right and top to bottom: engine performance variation as a function of mission parameters for configuration solution E.	50
4.10	From left to right and top to bottom: engine performance variation as a function of mission parameters.	51
4.11	From left to right and top to bottom: engine performance variation as a function of mission parameters.	53
4.12	Example of a sensitivity chart.	54
4.13	From left to right and top to bottom: engine performance variation as a function of engine components isentropic efficiency for case solution D.	55
4.14	From left to right and top to bottom: engine performance variation as a function of engine components isentropic efficiency for case solution E.	56
4.15	From left to right and top to bottom: engine performance variation as a function of engine components isentropic efficiency.	57
4.16	From left to right and top to bottom: engine performance variation as a function of engine components isentropic efficiency.	58
4.17	From left to right and top to bottom: engine performance variation as a function of engine components isentropic efficiency.	59

# List of Tables

2.1	Stages in a turbofan engine and its location.	8
3.1	Mission parameters under which optimization study is performed.	26
3.2	Other contextual parameters used in the study.	27
3.3	Lower and upper limits set for design parameters.	33
4.1	Key parameters of all solutions proposed as optimum configurations.	46
4.2	Deviation in performance parameters with respect to local optimums.	47



# Chapter 1

## Introduction

### 1.1 Incentive, justification and objectives

#### 1.1.1 Justification

In the field of commercial aviation, the efficient use of resources has become a key factor in the day-to-day life of airlines. One of the variables that is more present in this scenario is fuel consumption: the strict regulations that today regulate the emissions that an aircraft can generate causes airlines, and therefore manufacturers, to seek the production of eco-friendly engines with an increasingly reduced consumption.

In addition, the search for increasingly efficient engines has a double benefit for airlines provided that, the lower the fuel demanded by the aircraft, the lower the cost in this regard, and the greater the economic benefit that, let us not forget, is the *raison d'être* of any company.

For these reasons it is interesting to find engine configurations that reduce the specific consumption of the engine, without seeing its performance reduced in terms of thrust and always with a reasonable weight, as this factor is critical in any flying element.

#### 1.1.2 Incentive

Therefore, the objective of this work is to achieve an engine configuration that guarantees low fuel consumption, while powerful and light. Since these variables, as will be seen later, are at odds with each other, an intermediate solution that satisfies all requirements will be sought.

Since the type of engine currently prevailing is the turbofan type, the study focuses on this casuistry. The parameters that most influence performance will be searched for and an ideal combination that best meets the previously established requirements will be established.

#### 1.1.3 Objectives

Once both the aim and the excuses of this project have been set out, the following objectives have been established:

- On the one hand, the search of an turbofan engine configuration that minimises fuel consumption.
- On the other hand, checking that the selected configuration satisfies thrust and weight performances. Otherwise, a new full-satisfaction point has to be found.
- Study how the mission parameters set out for the study influence in the results obtained.

- Finally, results obtained must be compared with specialised literature in order to validate the proposal, as well as a discussion of them will be carried out.

# Chapter 2

## Theoretical background

### 2.1 Introduction

Throughout this chapter concepts the knowledge of which is necessary for a proper comprehension of this project are explained. Different types of jet engines are presented and the thermodynamic cycle that models the engine is developed and broken down. Finally, some performance parameters that permit the characterization of the whole are presented.

### 2.2 Gas turbine engines

#### General description

A gas turbine is defined as a continuous combustion, internal combustion engine. Internal combustion means that the engine carries out an energy conversion from chemical to thermal of the fluid that circulates through its core[5]. In the same way, continuous combustion signifies that the fluid is not stopped or retained to perform the energy exchange, but the process occurs while it is going on[2].

The operation of aerospace propulsion engines is based on Newton's laws of motion[3].

- The Second Newton's Law states that a change in the momentum of a body generates a force applied on it.
- The Third Newton's Law states that the force applied by a body exerts a reaction in terms of an equal and opposite direction force.

Moving these laws to the topic concerning this document, the force-applying body can be treated as a fluid circulating inside the engine whereas the air surrounding can be considered as the force-suffering one.

Generally, aerospace propulsion engines may be thought of as flow machines the fluid travelling in which is added heat and/or work prior to its exit as a jet. Thereby, thrust is produced according to the reaction principle. Indeed, such engines are often referred to as reaction engines.

#### 2.2.1 Classification

Once a gas turbine engine is defined, several classifications can be performed, attending to different criteria. In this document, a brief and general classification is published, just naming the main characteristics that separate one engine concept from the others.

The first distinction refers to the nature of the fluid the engine uses. If the machine gets the air from its surroundings, an air-breathing engine is given. On the contrary, if the engine manages the fluid to be used by itself, a rocket engine is got.

Next, regarding the fluid treatment inside the engine, the following classification is established:

- If the fluid is only given work, but no heat, a turboprop engine is got. In these type of engines thrust is performed by a propeller, whose spools create lift in the progress direction. As seen later, these kind of engines are very speed-limited, but very efficient.
- In the other hand, if heat is added to the airstream aboard, but no work is done on it, a jet engine is given. Thus, thrust is conducted by the emission of a high-speed exhaust jet, that has been burnt before. Although its efficiency is lower than turboprops', the speed range on which these engines can be used is much wider.

Concerning jet engines, a secondary classification can be carried out:

- In the case compression is performed automatically in the intake, a ramjet is given. These engines have the particular characteristic of lacking both compressor and turbine. Thrust is got when compressed, burnt air is expanded in a turbine. If the combustion takes place at a supersonic speed, a scramjet (or supersonic combustion ramjet) is yielded. Besides, if combustion occurs in pulses, a pulsejet engine appears. All these sort of engines need very high flying speeds so that air intaken is so energetic that a high compression occurs naturally.
- If a particular element is used to compress the airflow, a turbojet is given. In this case, air is taken up, then compressed before combustion. Then, flow expansion takes place in a turbine and finally expanded in a nozzle.

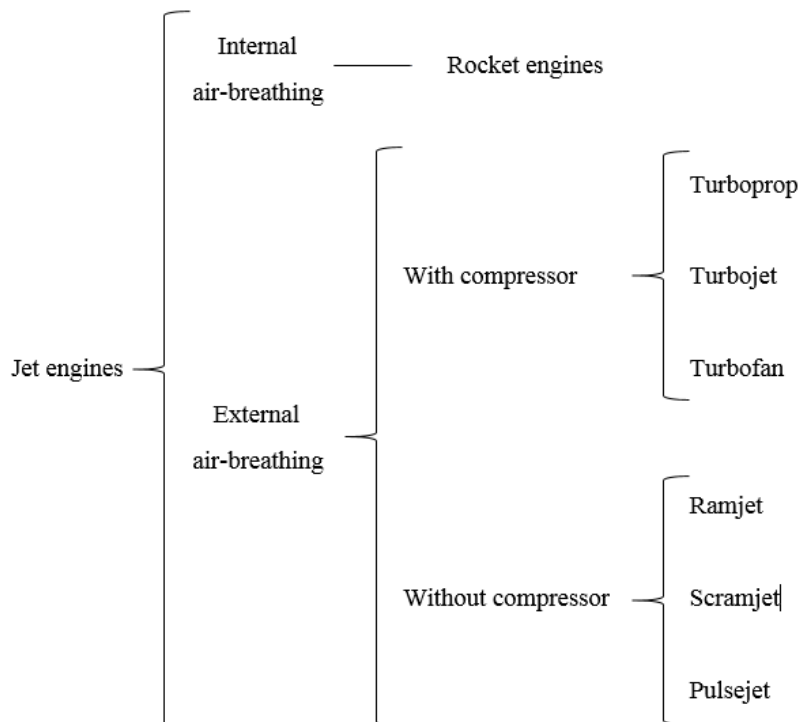


Figure 2.1: Draw of reaction engines classification.



### 2.2.2 The turbofan engine

When mixing both turboprop and turbojet engines, a turbofan arises. These configuration combines both concepts in order to get the benefits from the two.

Thus, in a turbofan engine fluid circulating is added both heat and work. Then, apart from all the components required to build a turbojet engine, it includes a secondary path around the core where air is just compressed and expanded. If this bypassed air is not reattached to the core-circulating air any more, a separated flow turbofan is got, whereas if both flows are joined affter the turbine, a mixed flow one is given. Figure 2.2 shows the typical configuration of a turbofan engine.

This project has been carried out only for unmixed flow turbofan engines.

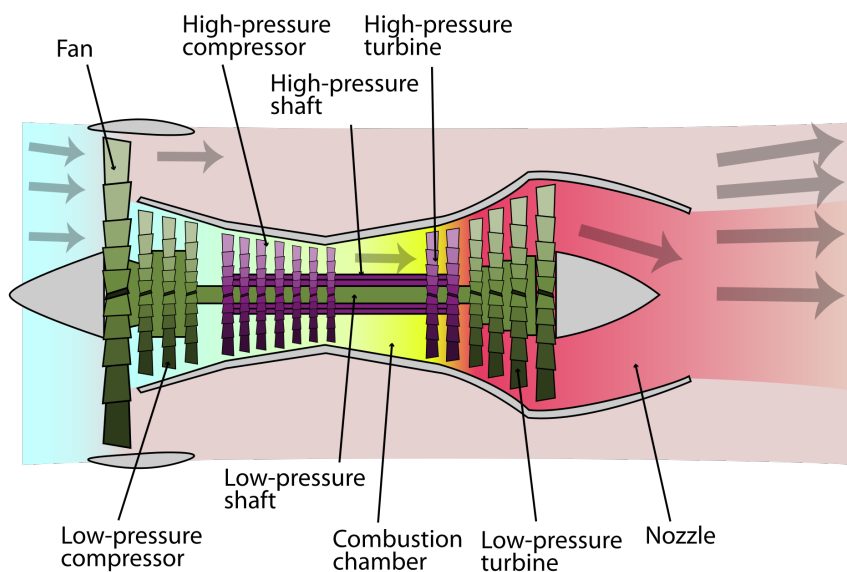


Figure 2.2: Diagram of a two-spool unmixed flow turbofan engine. Source:[1]

Briefly, these engines provide higher thrust and less consumption than turbofans, at subsonic speeds. Moreover, acoustic pollution can be reduced[2].

In the other hand, complexity of the system is higher, as well as the weight. Besides, these configuration is more exposed to impact of external objects such as ice.

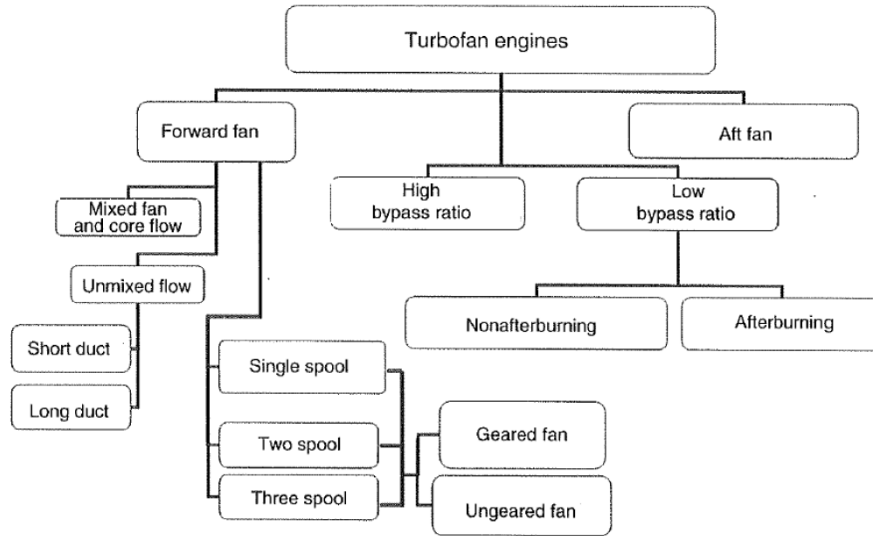


Figure 2.3: Turbofan engines classification, attending to different criteria. Source:[2]

### 2.2.3 Range of usage

Next, a brief explanation of each engine scope is conducted. Since turboprop engines use an airscrew to generate thrust, the speed at which they can work is limited to blade tip compressibility phenomena: the faster the aircraft is, the faster the spool spins, and then the propeller, resulting on a greater speed in blade tip, given a propeller diameter. As a consequence of this, flying a turboprop-driven aircraft at a relatively high speed turns unfeasible, since the efficiency of the propulsive plant would decrease resoundingly.

Turbojet engines, on the other hand, have a wider range of use because they do not have any propeller. The upper speed limit at which this type of engine should be used will in this case be marked by the intake system and the flow rate at this point, since in the case of highly hypersonic conditions it is preferable to eliminate the compressor and move to a ramjet configuration. Continuing with this analysis, these ramjet engines together with the scramjet are viable for a supersonic flight regime, otherwise the low speed at the entrance of the combustion chamber would make an efficient process impossible.

Finally, the rocket engines, given that they are autonomous in the supply of air, offer the possibility of working under any flight regime, from incompressible flow conditions to hypersonic regime.

A turbofan engine, on the other hand, is in the intermediate zone between a turbojet and a turboprop. The proximity to one or the other will depend on the amount of air passing through the combustion chamber and the secondary flow. This relationship can be computed, as shown below, using the parameter  $\beta$ , or BPR.

$$\beta = \frac{\dot{m}_\sigma}{\dot{m}_\pi} \quad (2.1)$$

In eq. 2.1,  $\dot{m}_\sigma$  refers to the airflow circulating around the combustion chamber whereas  $\dot{m}_\pi$  does to the one going through the engine core.

Figures 2.4 and 2.5 show the range of use of each engine configuration according to the flight speed.

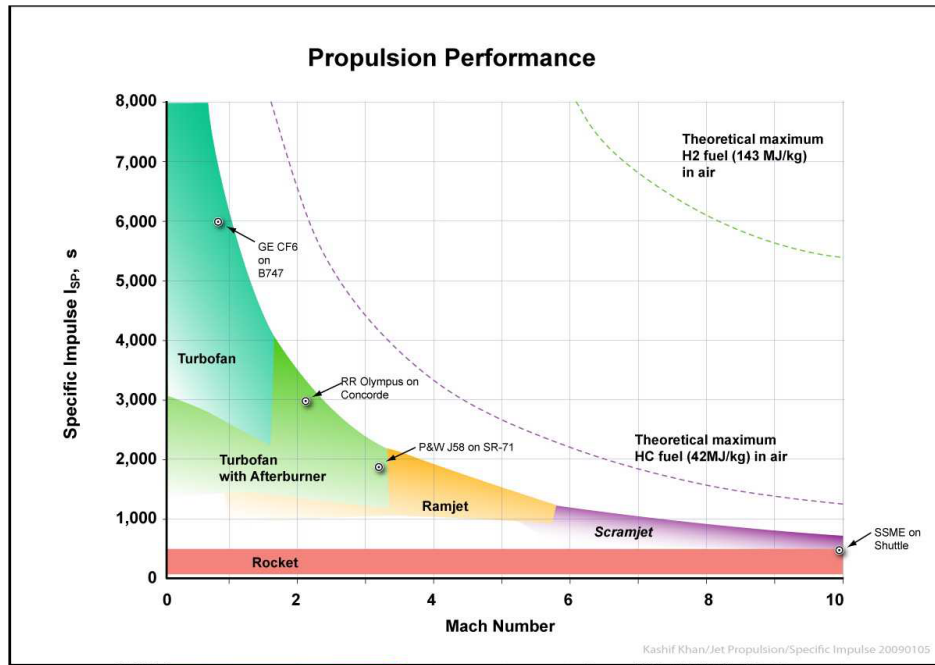


Figure 2.4: Aerospace jet engines applicability based on flight velocity and specific impulse. Specific impulse can be modeled, as a first approach, as the inverse of the specific fuel consumption. Source: [3].

As it can be seen, commercial applications, which require a high -but still subsonic- Mach number, may incorporate a turbofan engine to satisfy their requirements with a low consumption (or high specific impulse) demand. Provided that the study conducted in this project is focussed on the performance of the capabilities of commercial flights power plant, the study should be -and in the end it is- centered in the development of turbofan engines.

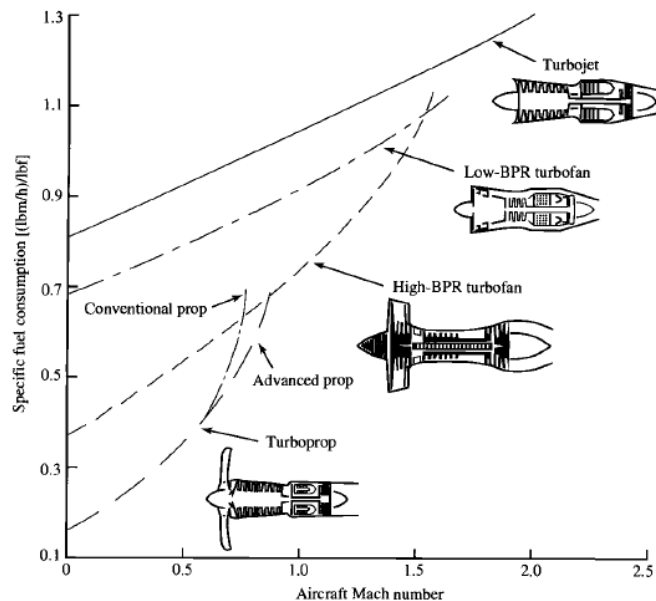


Figure 2.5: Aerospace jet engines applicability based on flight velocity and specific fuel consumption. Source: [4]

## 2.3 The Brayton cycle in a turbofan

Once the reason for studying turbofan engines is clear, a more detailed explanation, based on a thermodynamic evolution of the airflow, is developed throughout this section.

This cycle analysis aims the obtention of a first estimation of the engine performance, by means of some characteristic parameters. These parameters, whose definition is explained in section 2.4, mark the first iteration in the hole design of the whole.

The Brayton cycle is characterised by the presence of three components that modify the thermodynamic properties of the fluid it is working with[6]:

- A gas compressor.
- A burner (or combustion chamber).
- An expansion turbine.

Besides, a preliminary compression takes place during the air intake and a final expansion in a nozzle is performed in order to generate and direct the propulsive jet. These two stages are also considered as a part of the cycle. Each component is studied separately, and modeled as a black box in which only input and output parameters are given, with disregard of the process that internally occurs. Each intermediate point between two components is known as station. Table 2.1 shows the nomenclature used to name each station along the engine.

Stages of a turbofan	
Stage ID	Description
0	Farflow field
2	Intake end
21	Fan end - compressor start
3	Compressor end
4	Combustion end
41	High pressure turbine end
5	Fan turbine end
6	Afterburner end (if any)
9	Exhaust
19	Secondary exhaust

Table 2.1: Stages in a turbofan engine and its location.

Note that subindex  $t$  appears together with the identifying number. This is due to the use of static properties to perform calculations. This procedure must be carried out, provided that airflow energy the engine uses has not just a thermal nature, but also kinematic.

Brayton cycles are represented on a 2-D plot, whose x and y-axis are partially up to the user. Although a pressure-volume diagram is common in some cases, particularly when working with internal combustion engines, a temperature-entropy, or T-s graph will be used. Nonetheless, airflow pressure and temperature are set as the two working variables. Note that, once both are known, the obtention of density is immediate by applying the state equation (eq. 2.2), and so the entropy. Flow velocity will also be an important parameter, particularly at both ends of the cycle.

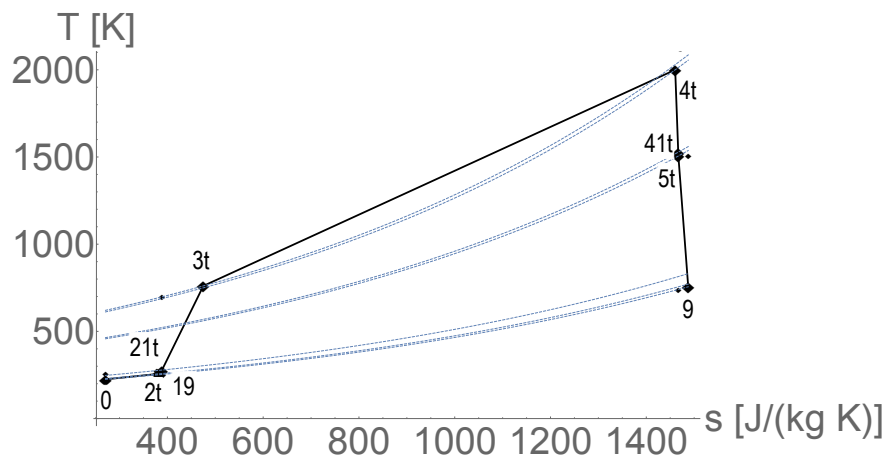


Figure 2.6: Brayton cycle in a turbofan engine.

### 2.3.1 Preliminary hypothesis

Before starting the cycle analysis, the hypothesis assumed for its development must be set. These assumptions, which try not to be so far from reality, aim the simplification of both the mathematical and computational processes. As it can be supposed, the more precision in the results required, the less hard hypothesis can be set. As a first approach, the calculation of the engine performance through the Brayton cycle use these hypothesis:

- The working fluid is a perfect gas, thus, it accomplishes with the ideal gas law (eq. 2.2 and the specific heat at a constant pressure,  $c_p$ , remains constant, whatever the temperature.

$$p = \rho \cdot R \cdot T \quad (2.2)$$

- Friction losses between airflow and engine walls are negligible.
- Mechanical losses in the shaft are not considered.
- No flow is bypassed in the middle of the cycle. This assumption is far from reality, since all engines use some of the air absorbed to refrigerate the hottest components (i.e. the turbine entrance) and the living space (air conditioning). Nonetheless, if the quantity of bypassed air is low (and in fact, it is), engine performance does not vary significantly. This practice, now unexisting, is known as air bleeding.
- No change in neither physical and chemical properties of the fluid is given.
- Combustion is supposed to be instantaneous and complete. According to this hypothesis, no products such as  $\text{NO}_x$  and unburnt hydrocarbons are emitted. Although is well known that it does not represent real cases, the negligence of engine emissions does not modify results obtained.
- Finally, steady flow is assumed.

Any cycle accomplishing with these assumptions will be considered a “real” cycle, whereas an “ideal” cycle also fulfills these statements:

- All compression processes are isentropic.

- All expansion processes are isentropic.
- Isobaric combustion.

### 2.3.2 Intake

The intake is the process in which air is absorbed and diffused by the engine and directed towards the core. It is composed on a rotating fan whose function is to enclose the mass airflow that will go through the engine, as well as perform a first compression, not high in the case of a turbofan.

To model this component, farflow conditions are considered as input, whereas conditions at the compressor entrance are set as output.

$$\{M_0, T_0, p_0\} \longrightarrow \{T_{2t}, p_{2t}\}$$

First of all, transition from dynamic to stagnation conditions must be done. To do so, wide known eqs. 2.3 can be used.

$$\begin{aligned} T_{0t} &= T_0 \left( 1 + \frac{\gamma - 1}{2} M_0^2 \right) \\ p_{0t} &= p_0 \left( 1 + \frac{\gamma - 1}{2} M_0^2 \right)^{\frac{\gamma - 1}{\gamma}} \end{aligned} \quad (2.3)$$

Note that, if no velocity is got (i.e. an engine bank) both points coincide.

Diffusion is performed throughout an adiabatic process, then, the static temperature during air compression remains constant.

$$T_{2t} = T_{0t} \quad (2.4)$$

If diffusor is considered as ideal, no pressure losses are given during the process. However, in real cycles, this issue must be considered. The main parameter modelling this loss is the diffusor isentropic efficiency, that compares the entalpy step in a real case with the one ideally got:

$$\eta_d = \frac{h_{2ts} - h_0}{h_{2t} - h_0} \quad (2.5)$$

where the subindex  $_s$  refers to conditions of the hypothetical isentropic process.

Considering perfect gas and dividing by  $T_0$ , eq. 2.5 turns:

$$\eta_d = \frac{\frac{T_{2ts}}{T_0} - 1}{\frac{T_{2t}}{T_0} - 1} \quad (2.6)$$

Denominator of 2.6 can be easily found from eq. 2.3. Also, points  $2ts$  and  $0$  have the same entropy, so isentropic relation 2.7 can be applied to this particular case:

$$p^{1-\gamma} T^\gamma = const. \longrightarrow \frac{T_{2ts}}{T_0} = \left( \frac{p_{2ts}}{p_0} \right)^{\frac{\gamma-1}{\gamma}} \quad (2.7)$$

So, eq. 2.6 can be written as:

$$\eta_d = \frac{\left( \frac{p_{2ts}}{p_0} \right)^{\frac{\gamma-1}{\gamma}} - 1}{\frac{\gamma-1}{2} M_0^2} \quad (2.8)$$

where isobar between  $2t$  and  $2ts$  conditions has been considered. Solving  $p_{2t}$ :

$$p_{2t} = p_{0t} \left( 1 + \frac{\gamma - 1}{2} M_0^2 \eta_d \right)^{\frac{\gamma}{\gamma - 1}} \quad (2.9)$$

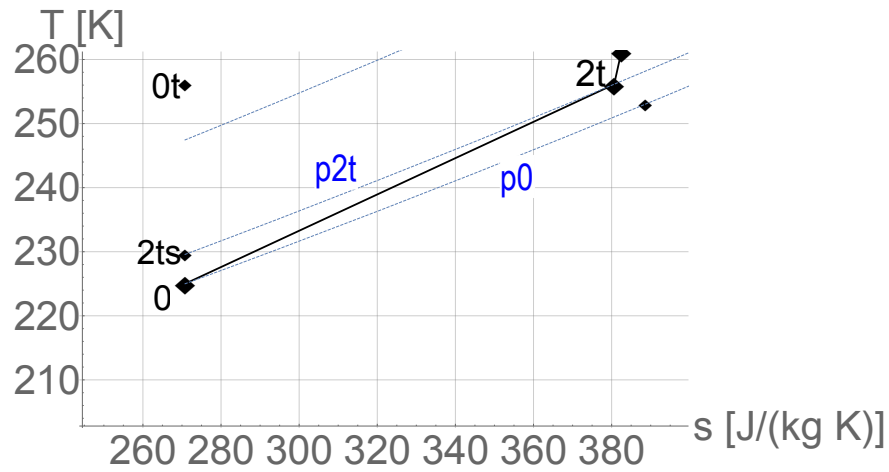


Figure 2.7: Detail of the intake part in the Brayton cycle.

### 2.3.3 Fan

Fan is one of the characteristic parts of a turbofan engine: its mission is to compress the flow that will be bypassed before the compressor entrance. Unlike the compressor, a fan incorporates few stages.

Airflow is taken from the diffuser, compressed and heated, and then separated before entering the compressor. Although the main aim is to treat the secondary flow, mainflow is also circulating and so compressed.

$$\{T_{2t}, p_{2t}\} \longrightarrow \{T_{21t}, p_{21t}\}$$

The procedure for the obtention of the output parameters is analogue to the one shown for the compressor in section 2.3.4. In fact, there is no difference among them, but it is incorporated to enable a separated compression of both flows.

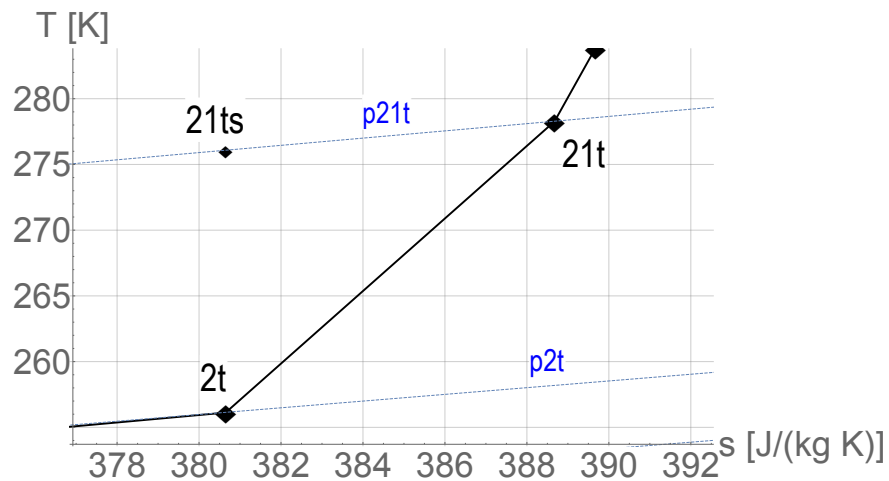


Figure 2.8: Detail of the fan part in the Brayton cycle.

### 2.3.4 Compressor

Compressor is one of the main components of a Brayton cycle. It composes, together with the combustion chamber and the turbine, the engine core. This is a complex -and critical- part of the engine, and it is composed by compression stages, each one of them composed, in turn, by a stator and a rotor.

Nevertheless, as commented before, the internal behaviour of the compressor is not studied, and thus an overall compression is computed.

In this part, points at the beginning of compression and combustion are taken as input and output, respectively.

Note that an engine can incorporate more than one turbine-compressor set in order to increase the efficiency. This is not the case since a single-spool engine has been modelled, but, if not, intermediate stations between 2 and 3 should be named (i.e. 25 for a two-spool engine or 23 and 27 for a three-spool).

$$\{T_{21t}, p_{21t}\} \longrightarrow \{T_{3t}, p_{3t}\}$$

The compression capacity of the system is given in datasheets. This magnitude, known as pressure ratio, or  $\beta_c$ , is commonly used as a performance parameter of the compressor.

$$\beta_c = \frac{p_{3t}}{p_{21t}} \quad (2.10)$$

then, pressure at the exit can be easily obtained.

$$p_{3t} = p_{21t} \cdot \beta_c \quad (2.11)$$

To obtain the temperature at the exit, more information is needed: just like the intake, an isentropic efficiency is defined for the compressor in a non ideal cycle:

$$\eta_c = \frac{h_{3ts} - h_{21t}}{h_{3t} - h_{21t}} \quad (2.12)$$

Again, applying perfect gas hypothesis:

$$\eta_c = \frac{T_{3ts} - T_{21t}}{T_{3t} - T_{21t}} \quad (2.13)$$

Solving  $T_{3t}$  and applying  $T_{21t}$  as common factor:

$$T_{3t} = T_{21t} + \frac{T_{3ts} - T_{21t}}{\eta_c} = T_{21t} \left( 1 + \frac{T_{3ts} - 1}{\eta_c} \right) \quad (2.14)$$

Note that  $3ts$  and  $2t$  are isentropic stations, by definition. Then, the following relationship can be applied, as done in 2.7:

$$\frac{T_{3ts}}{T_{21t}} = \frac{p_{3ts}}{p_{21t}}^{\frac{\gamma-1}{\gamma}} = \beta_c^{\frac{\gamma-1}{\gamma}} \quad (2.15)$$

where isobaric conditions between  $3t$  and  $3ts$  have been considered.

Finally, compressor exit temperature can be solved by adding 2.15 into 2.14

$$T_{3t} = T_{21t} \left( 1 + \frac{\beta_c^{\frac{\gamma-1}{\gamma}} - 1}{\eta_c} \right) \quad (2.16)$$



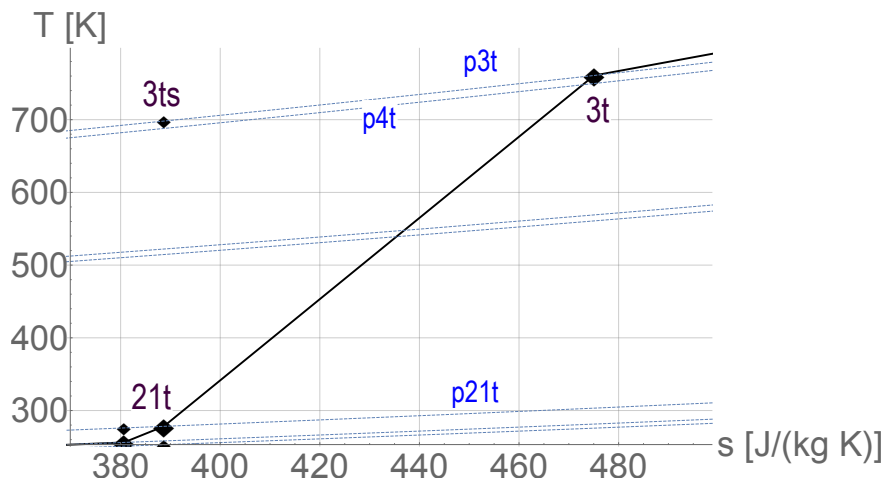


Figure 2.9: Detail of the compression part in the Brayton cycle.

### 2.3.5 Combustion chamber

The combustion chamber is the engine component where combustion takes place. As known, this is a complex unsteady process, in which both chemical equilibrium and kinetics take an important role. A complete combustion model requires a wide knowledge of the process as well as a high computational effort. For this reasons, the phenomenon must be simplified. In this case, no intermediate reactions have been considered, but a macroscopic energy balance has been conducted. Also, as mentioned in the hypothesis, all fuel is supposed to burnt perfectly.

In other words, the combustion chamber is a closed area where fuel is added and the temperature of the mixture is risen. Moreover, in the case of a real cycle, a pressure loss will be got.

$$\{T_{3t}, p_{3t}\} \longrightarrow \{T_{4t}, p_{4t}, f\}$$

Note that a new output appears:  $f$ , named as fuel-to-air ratio, measures the quantity of fuel that is added to the airflow for the combustion, in terms of massflow.

$$f = \frac{\dot{m}_f}{\dot{m}_a} \quad (2.17)$$

Actually, the variable  $T_{4t}$ , although should be calculated by applying combustion laws, is fixed by the designer. In this way, it becomes an input and the quantity of fuel burnt, represented by  $f$ , is not controlled but dominated by  $T_{4t}$ . Companies try to maximize this parameter, since the higher temperature combustion takes place, the higher the thermal efficiency is. However, materials engineering existing today do not allow to work with such high temperatures. Hence, it will be limited by the manufacturer capacity of building tough materials as well as performing a good refrigeration system.

Thermodynamically, the combustion can be treated, in a very simple way, as a process where some thermal energy is added to the fluid, suffering a little pressure loss.

Pressure losses during combustion are usually oputed via the pneumatic efficiency of the combustor,  $\eta_{pc}$ :

$$\eta_{pc} = \frac{p_{4t}}{p_{3t}} \quad (2.18)$$

So, pressure at the end of the chamber can be easily obtained:

$$p_{4t} = p_{3t} \cdot \eta_{pc} \quad (2.19)$$

Now, an energetic balanced is conducted: enthaply of the incoming flow must be equal to the one outgoing, when fuel energy is added. In this way, equation 2.20 can be established:

$$\dot{m}_a c_p T_{3t} + \eta_b \dot{m}_f Q_f = (\dot{m}_a + \dot{m}_f) c_p T_{4t} \quad (2.20)$$

where  $Q_f$  is the heat of combustion of the fuel, that is, energy released by fuel uint of mass. Moreover, the parameter  $\eta_c$  refers to the combustion process efficiency.

dividing by  $\dot{m}_a$ :

$$c_p T_{3t} + \eta_b \frac{\dot{m}_f}{\dot{m}_a} Q_f = \left(1 + \frac{\dot{m}_f}{\dot{m}_a}\right) c_p T_{4t} \quad \rightarrow \quad c_p T_{3t} + \eta_b f Q_f = (1 + f) c_p T_{4t} \quad (2.21)$$

Finally, solving  $f$ :

$$f = \frac{c_p (T_{4t} - T_{3t})}{\eta_c Q_f - c_p T_{4t}} \quad (2.22)$$

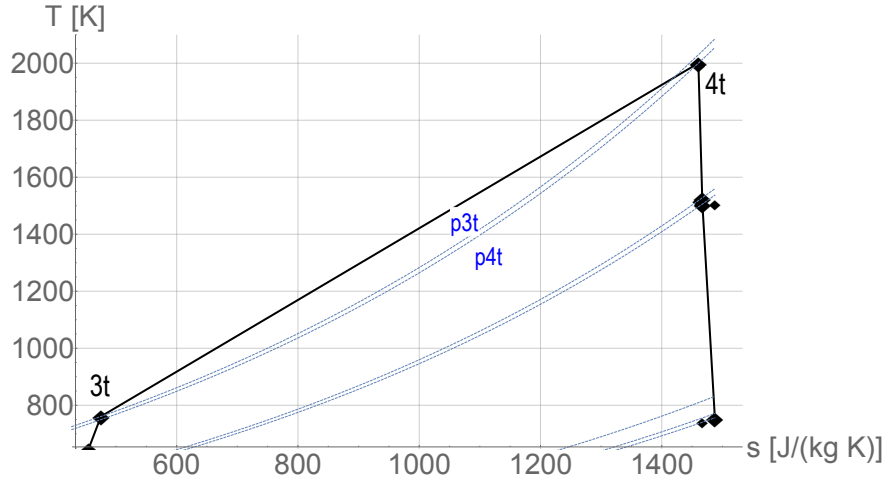


Figure 2.10: Detail of the combustion in the Brayton cycle.

### 2.3.6 Turbine

In a turbine, air is expanded. The mission of the turbine is to spin the compressor through the spool connecting them.

During this stage, air is cooled, and energy produced is consumed by the compressor. However, the divergence that exists between isobars in the diagram show that a residual amount of energy stays uncomsumed. This quantity is leveraged in the nozzle and, as a last resort, is the one that generates thrust.

$$\{T_{4t}, p_{4t}\} \quad \longrightarrow \quad \{T_{41t}, p_{41t}\}$$

Provided that the turbine feeds the compressor, there must be a balance in the energy consumption. So, equation 2.23 can be established:

$$\Delta h_t = \Delta h_c \quad \longrightarrow \quad c_p (T_{3t} - T_{2t}) = \eta_m (1 + f) c_p (T_{4t} - T_{41t}) \quad (2.23)$$

where  $\eta_m$  models mechanical losses during energy transmission in the spool. Note that fuel adding has been included by using  $f$ .

Solving  $T_{41t}$ :

$$T_{41t} = T_{4t} - \frac{1}{\eta_m} \frac{T_{3t} - T_{21t}}{1 + f} \quad (2.24)$$

Now, as done during compression, an isentropic efficiency is defined. In this case, the ideal case considers the maximum expansion, that in real cases is less.

$$\eta_t = \frac{h_{1t} - h_{41t}}{h_{4t} - h_{41ts}} \quad (2.25)$$

considering a perfect gas:

$$\eta_t = \frac{T_{4t} - T_{41t}}{T_{4t} - T_{41ts}} \quad (2.26)$$

Solving  $T_{41t}$ :

$$T_{41ts} = T_{4t} - \frac{T_{4t} - T_{41t}}{\eta_t} = T_{4t} \left( 1 - \frac{\frac{T_{5t}}{T_{4t}} - 1}{\eta_t} \right) \rightarrow \frac{T_{5ts}}{T_{4t}} = \frac{T_{4t} - T_{41t}}{\eta_t} = T_{4t} \left( 1 - \frac{\frac{T_{5t}}{T_{4t}} - 1}{\eta_t} \right) \quad (2.27)$$

Knowing that points  $4t$  and  $5ts$  are isentropic:

$$\frac{T_{41ts}}{T_{4t}} = \left( \frac{p_{41ts}}{p_{4t}} \right)^{\frac{\gamma}{\gamma-1}} \quad (2.28)$$

substituting 2.28 in 2.27:

$$\left( \frac{p_{41t}}{p_{4t}} \right)^{\frac{\gamma}{\gamma-1}} = \frac{T_{4t} - T_{41t}}{\eta_t} = T_{4t} \left( 1 - \frac{\frac{T_{41t}}{T_{4t}} - 1}{\eta_t} \right) \quad (2.29)$$

where isobaric conditions between  $5ts$  and  $5t$  have been considered.

finally, solving  $p_{41t}$ , we obtain:

$$p_{41t} = p_{4t} \left[ 1 - \frac{1}{\eta_t} \left( 1 - \frac{T_{41t}}{T_{4t}} \right) \right]^{\frac{\gamma}{\gamma-1}} \quad (2.30)$$

Note that, in the case of a two (or three) spool engine, this procedure should be repeated for any turbine-compressor union, including in the energy balance all components connected to the same spool.

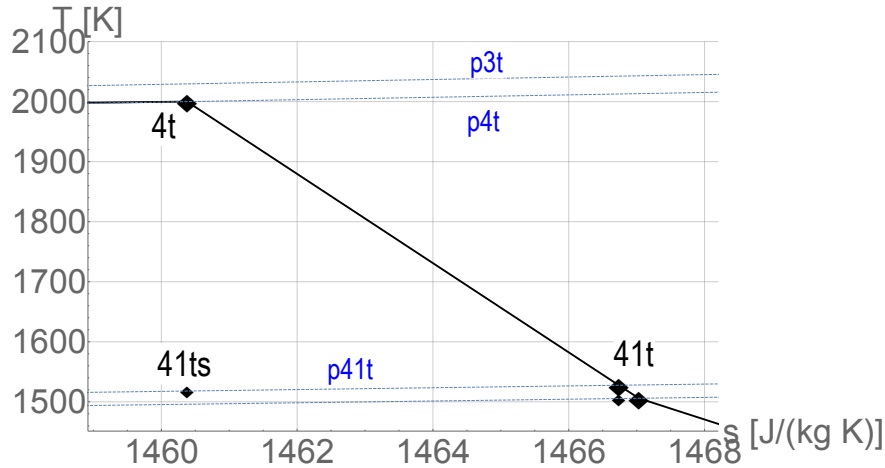


Figure 2.11: Detail of the high pressure turbine in the Brayton cycle.

### Fan turbine

The fan turbine is the component that spins the fan. In a single-spool engine, it can be also named low pressure turbine. It works with primary flow only and is located after the main -or high pressure- turbine that moves the compressor. The exit is connected to the afterburner or, in the case there is not, to the nozzle.

$$\{T_{41t}, p_{41t}\} \longrightarrow \{T_{5t}, p_{5t}\}$$

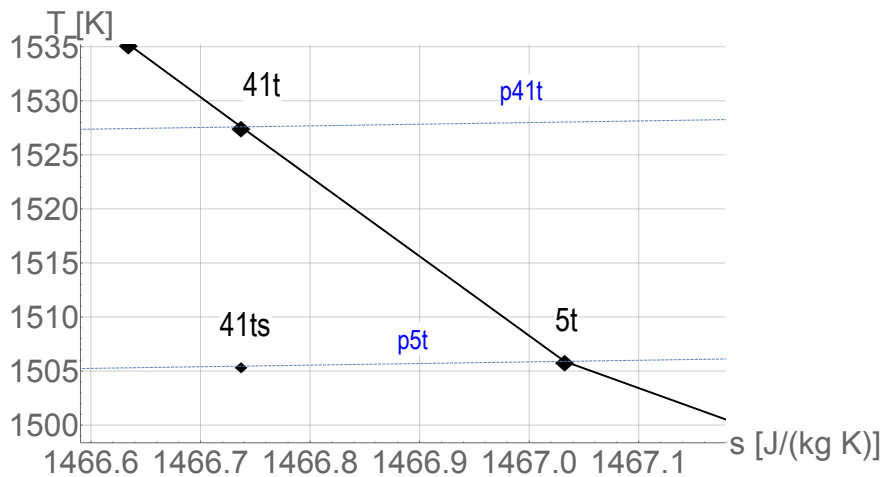


Figure 2.12: Detail of the fan turbine in the Brayton cycle.

### 2.3.7 Afterburner

The afterburner is a secondary chamber where airflow is reburnt. This is one of the most popular thrust increasing mechanisms. However, it is only used for military applications ,where extra immediate thrust may be demanded. In commercial aviation, on its hand, this system is not incorporated to the engine, since specific combustion rises exponentially. Therefore, provided that the objective of this project is, among others, the reduction of this parameter, the afterburner

system will not be studied. Nonetheless, the procedure for solving this component is analogue to the one shown in 2.3.4.

### 2.3.8 Nozzle

The nozzle is the last component of a Brayton cycle. In it, remaining energy on the turbine exit is used via the emission of a very quick jet.

In this case, the analysis is a little bit deeper: apart from obtaining pressure and temperature conditions at the exit, the evaluation of the jet velocity is also important, since it marks the thrust the engine can perform. Moreover, the velocity of the airflow determines the kind of nozzle to be used (convergent or convergent-divergent) and the possibility of flow shocking must be considered.

$$\{T_{5t}, p_{5t}\} \longrightarrow \{T_9, p_9 M_9\}$$

Note that, since this is the end of the engine, dynamic conditions are obtained in the output. First, the isentropic efficiency of the nozzle is defined, as follows:

$$\eta_n = \frac{h_{5t} - h_9}{h_{5t} - h_{9s}} = \frac{T_{5t} - T_9}{T_{5t} - T_{9s}} \quad (2.31)$$

where gas perfect hypothesis has been applied. Dividing by  $T_{5t}$ :

$$\eta_n = \frac{1 - \frac{T_9}{T_{5t}}}{1 - \frac{T_{9s}}{T_{5t}}} \quad (2.32)$$

Considering the expansion process in the nozzle as adiabatic, no temperature change is got, so  $T_{9t} = T_{5t}$ , and:

$$\eta_n = \frac{1 - \frac{T_9}{T_{9t}}}{1 - \frac{T_{9s}}{T_{9t}}} \quad (2.33)$$

Knowing 9t and 9s are isentropic stations:

$$\eta_n = \frac{1 - \left(\frac{p_9}{p_{9t}}\right)^{\frac{\gamma-1}{\gamma}}}{1 - \left(\frac{p_9}{p_{5t}}\right)^{\frac{\gamma-1}{\gamma}}} \quad (2.34)$$

Solving:

$$\frac{p_9}{p_{9t}} = \left[ 1 - \eta_n \left\{ 1 - \left(\frac{p_9}{p_{5t}}\right)^{\frac{\gamma-1}{\gamma}} \right\} \right]^{\frac{\gamma}{\gamma-1}} \quad (2.35)$$

Rewriting  $\frac{p_{5t}}{p_{9t}} = \frac{p_9}{p_{9t}} \cdot \frac{p_{5t}}{p_9}$ , the stagnation pressure ratio in the nozzle is obtained:

$$\frac{p_{5t}}{p_{9t}} = \frac{p_{5t}}{p_9} \left[ 1 - \eta_n \left\{ 1 - \left(\frac{p_9}{p_{5t}}\right)^{\frac{\gamma-1}{\gamma}} \right\} \right]^{\frac{\gamma}{\gamma-1}} \quad (2.36)$$

Next, the exhaust velocity in the nozzle is obtained:

$$V_9 = \sqrt{2(h_{5t} - h_9)} = \sqrt{2\eta_n(h_{5t} - h_{9s})} = \sqrt{2c_p\eta_n(T_{5t} - T_9)} = \sqrt{2c_p\eta_n T_{5t} \left[ 1 - \left(\frac{p_9}{p_{5t}}\right)^{\frac{\gamma-1}{\gamma}} \right]} \quad (2.37)$$

where eq. 2.31 and perfect gas assumption have been used. Then, Mach number at the exit can be calculated as:

$$M_9^2 = \frac{V_9^2}{\gamma R T_9} \quad (2.38)$$

bearing in mind that:

$$\frac{T_{9t}}{T_9} = 1 + \frac{\gamma - 1}{2} M_9^2 = \frac{T_{5t}}{T_9} \quad (2.39)$$

Combining eqs. 2.37 and 2.38:

$$M_9^2 = \frac{2}{\gamma - 1} \eta_n \frac{T_{5t}}{T_9} \left[ 1 - \left( \frac{p_9}{p_{5t}} \right)^{\frac{\gamma-1}{\gamma}} \right] \quad (2.40)$$

substituting 2.39 in 2.40:

$$M_9^2 = \frac{2}{\gamma - 1} \eta_n \left( 1 + \frac{\gamma - 1}{2} M_9^2 \right) \frac{T_{5t}}{T_9} \left[ 1 - \left( \frac{p_9}{p_{5t}} \right)^{\frac{\gamma-1}{\gamma}} \right] \quad (2.41)$$

finally, solving  $M_9^2$ :

$$M_9^2 = \frac{2}{\gamma - 1} \left[ \frac{\eta_n \left[ 1 - \left( \frac{p_9}{p_{5t}} \right)^{\frac{\gamma-1}{\gamma}} \right]}{1 - \eta_n \left[ 1 - \left( \frac{p_9}{p_{5t}} \right)^{\frac{\gamma-1}{\gamma}} \right]} \right] \quad (2.42)$$

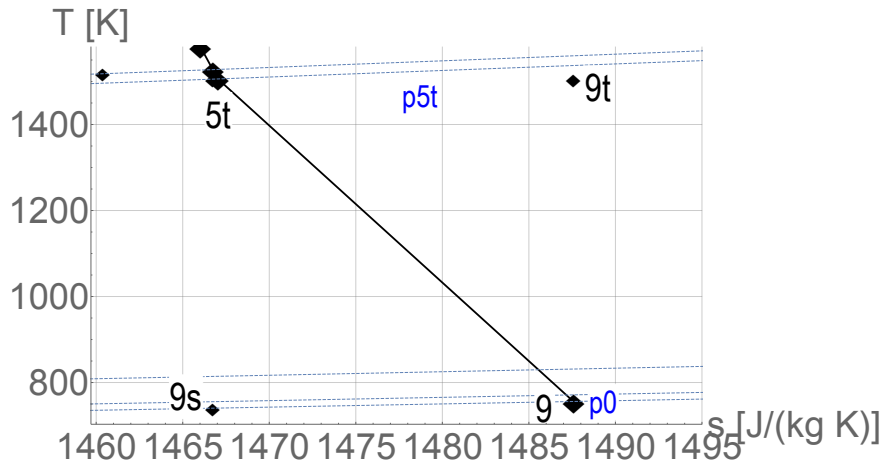


Figure 2.13: Detail of the primary nozzle in the Brayton cycle.

### Critical conditions review

Once Mach in the nozzle is set, a study of the flow conditions inside this component is conducted. Provided that flow suffers an acceleration during its circulation along the nozzle, supersonic flow can be reached at the end of this component. If so, the flow is said to be in “critical conditions”. If the geometry of the duct is not changed, no more acceleration is got, and flow stays unchanging. When this happens, the nozzle is “shocked” and no more pressure decrease is given.

The evaluation of this critical pressure is important since, if it is different from air pressure outside the engine, a shock wave appears. This is an undesirable effect provided that thrust is not so high and drag increases.

So, by stating  $M_9^2 = 1$  in eq. 2.42, critical pressure can be obtained:

$$\frac{p_{6t}}{p^*} = \frac{1}{\left(1 - \eta_n \frac{\gamma-1}{\gamma+1}\right)^{\frac{\gamma}{\gamma-1}}} \quad (2.43)$$

This value must be compared with ambient pressure,  $p_0$ . Two possible cases may happen:

- If  $p^* \geq p_0$ , nozzle is choked, pressure at the exit is equal to the critical pressure,  $p_9 = p^*$ , and  $M_9 = 1$ . Besides:

$$T_{5t} = T_9 \left(1 + \frac{\gamma-1}{2} M_9^2\right) \quad \longrightarrow \quad T_9 = \frac{2}{\gamma-1} T_{5t} \quad (2.44)$$

- If  $p^* < p_0$ , nozzle is adapted, so:

$$T_9 = T_{5t} \left\{ 1 - \eta_n \left[ 1 - \left( \frac{p_9}{p_{5t}} \right)^{\frac{\gamma-1}{\gamma}} \right] \right\} \quad (2.45)$$

$$V_9 = \sqrt{2 c_p (T_{5t} - T_9)}$$

To adapt the flow a convergent-divergent nozzle must be used; in this way, flow will adjust so that critical conditions are got in the throat, then accelerated in the divergent part, while pressure decreases until ambient conditions.

### 2.3.9 Bypassed flow

Flow that is not circulating through the core, but bypassed around the compressor-combustor-turbine set, experiments a different thermodynamic path before its expulsion in the nozzle.

After compression in the fan is carried out, flow is directly expanded in a secondary nozzle. The procedure is similar to the one shown in section 2.3.8. Although the same theory can be applied, no shocking flow is got, provided that flow speed is in this case much lower.

Hence, the conditions at the exit of the secondary exhaust are the following:

$$p_{19} = p_0 \quad (2.46)$$

$$T_{19} = T_{21t} \left\{ 1 - \eta_n \left[ 1 - \left( \frac{p_{19}}{p_{21t}} \right)^{\frac{\gamma-1}{\gamma}} \right] \right\} \quad (2.47)$$

$$V_{19} = \sqrt{2 c_p (T_{21t} - T_{19})} \quad (2.48)$$

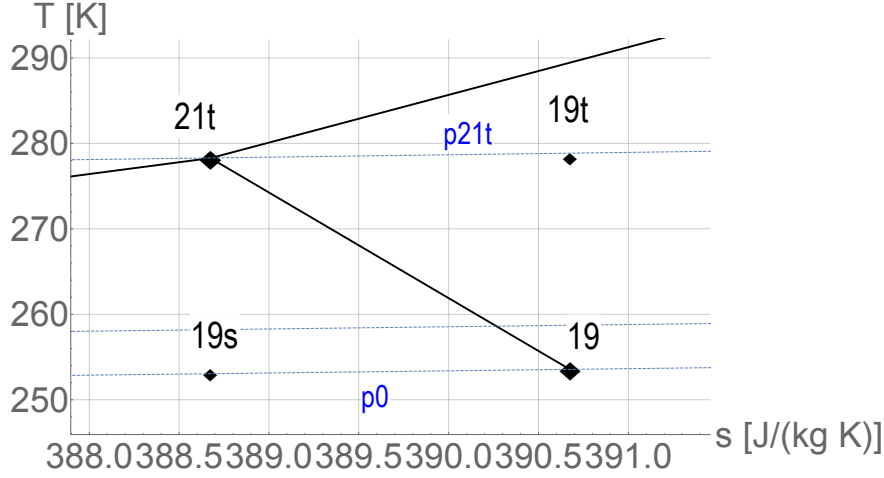


Figure 2.14: Detail of the secondary nozzle in the Brayton cycle.

## 2.4 Engine performance

Performance parameters are essential because they quantify the quality of a jet engine. In a turbofan, the most popular performance parameters are presented throughout this section.

### 2.4.1 Specific thrust

Thrust in an engine arises when fluid through the engine increases its motion quantity. In a jet engine, thrust is calculated by using eq. 2.49.

$$T = \dot{m}_a [(1 + f) V_9 - V_0] + (p_9 - p_0) A_9 \quad (2.49)$$

Note that, in a turbofan engine, this expression refers only to the flow going through the core. When the contribution of the secondary nozzle is added, eq. 2.49 changes as follows:

$$T = \dot{m}_a [(1 + f) V_9 - V_0] + \dot{m}_a \beta [V_{19} - V_0] + (p_9 - p_0) A_9 + (p_{19} - p_0) A_{19} \quad (2.50)$$

The fluid is touching the internal walls of the engine. Thus, both pressure and friction forces appear[7]. As a consequence, drag is generated inside the engine. This negative contribution should be added to the previous expression, together with the drag the engine itself produces when is in contact with ambient air. If so, engine thrust becomes:

$$T_{ins} = T - D_{ext} - D_{ad} \quad (2.51)$$

where  $D_{ext}$  and  $D_{ad}$  refer to external and additional drag inside, respectively.

Thrust in 2.51 is usually called installed thrust, whereas the one calculated in 2.49 is net thrust. Note that, if both nozzles are adapted, 2.49 can be simplified:

$$T = \dot{m}_a [(1 + f) V_9 - V_0] + \dot{m}_a \beta [V_{19} - V_0] \quad (2.52)$$

even, considering fuel flow is negligible compared to air flow:

$$f \ll 1 \quad \longrightarrow \quad T = \dot{m}_a (V_9 - V_0) + \dot{m}_a \beta (V_{19} - V_0) \quad (2.53)$$

Note that high thrust can be obtained by following two strategies:



- Circulating a high mass flow, which characterises turbofan engines.
- Performing a high velocity in the exhaust gases, which is typical from turbojet engines.

Specific magnitudes refer to a magnitude divided by the mass, commonly. In this case, specific thrust is defined as the ratio between thrust and massflow. However, several massflows appear in a turbofan. The most common procedure to get an specific thrust is to divide thrust by the total airflow:

$$TS = \frac{(1 + f) V_9 - V_0 + \beta (V_{19} - V_0) + \frac{A_9}{\dot{m}_\pi} (p_9 - p_0) + \frac{A_{19}}{\dot{m}_\pi} (p_{19} - p_0)}{1 + \beta} \quad (2.54)$$

where specific areas can be calculated by applying massflow definition:

$$\begin{aligned} \dot{m}_9 = \rho_9 V_9 A_9 &\rightarrow \frac{a_9}{\dot{m}_9} = \frac{1}{\rho_9 V_9} \\ \dot{m}_{19} = \dot{m}_9 \beta = \rho_{19} V_{19} A_{19} &\rightarrow \frac{A_9}{\dot{m}_{19}} = \frac{\beta}{\rho_{19} V_{19}} \end{aligned} \quad (2.55)$$

### 2.4.2 Specific consumption

Consumption in a vehicle is defined as the quantity of fuel it uses to provide a certain amount of energy. Applied to a jet engine, energy becomes thrust, and fuel is used in terms of massflow. Therefore, the thrust specific fuel consumption is defined as shown below:

$$TSFC = \frac{\dot{m}_f}{T} \quad (2.56)$$

dividing by primary air flow:

$$TSFC = \frac{\dot{m}_f / \dot{m}_\pi}{T / \dot{m}_\pi} = \frac{f}{TS} \quad (2.57)$$

### 2.4.3 Specific impulse

This magnitude quantifies thrust obtained by unit of fuel consumption[7].

$$I_s = \frac{T}{\dot{m}_f g} \quad (2.58)$$

again, dividing 2.58 by  $\dot{m}_\pi$ :

$$I_s = \frac{1}{TSFC g} \quad (2.59)$$

### 2.4.4 Thermal efficiency

This parameters relies to cycle performance, rather than for the whole engine. It can be defined as the quotient among useful work obtained and heat added during combustion[7]. Eq. 2.60 shows the mathematical expression for this statement.

$$\eta_{th} = \frac{(h_{5t} - h_9) - (h_{2t} - h_0)}{h_{4t} - h_{3t}} = \frac{(T_{5t} - T_9) - (T_{2t} - T_0)}{(T_{4t} - T_{3t})} \quad (2.60)$$

Another approach is to consider the jet engine as an energy converter, from chemical to kinetic. Thus, the thermal efficiency of a turbofan engine can be expressed as follows[7]:

$$\eta_{th} = \frac{\Delta E_{c\pi} + \Delta E_{c\sigma}}{\dot{m}_f L} = \frac{\frac{1}{2} \dot{m}_a (1+f) V_9^2 - \frac{1}{2} \dot{m}_a V_0^2}{\dot{m}_f L} = \frac{\frac{1}{2} \dot{m}_\pi [(1+f) V_9^2 - V_0^2] + \frac{1}{2} \dot{m}_\sigma (V_{19}^2 - V_0^2)}{\dot{m}_f L} \quad (2.61)$$

A simplification of this expression can be performed by neglecting fuel contribution and dividing the whole by the core airflow:

$$\eta_{th} = \frac{V_9^2 + \beta V_{19}^2 - (1+\beta) V_0^2}{2fL} \quad (2.62)$$

### 2.4.5 Propulsive efficiency

This parameter refers to the engine capacity for performing a good jet.

If exhaust gases are emitted at a speed  $V_9$ , but the aircraft is flying only at  $V_0$ , some energy is lost in the process. In other words, fluid flow is heated uselessly. Then, propulsive efficiency quantifies this loss, compared with energy given to the aircraft.

$$\begin{aligned} \eta_p &= \frac{V_0 T}{V_0 T + P_{loss}} = \\ &= \frac{V_0 [\dot{m}_\pi \{(1+f) V_9 - V_0\} + A_9 (p_9 - p_0) + \dot{m}_\sigma (V_{19} - V_0) + A_{19} (p_{19} - p_0)]}{V_0 T + \frac{1}{2} \dot{m}_\pi (1+f) (V_9 - V_0)^2 + \frac{1}{2} \dot{m}_\sigma (V_{19} - V_0)^2} \end{aligned} \quad (2.63)$$

If nozzle is adapted and fuel flow is neglected, eq. 2.63 can be simplified:

$$\eta_{prop} = \frac{2V_0 (V_9 + \beta V_{19} - (1+\beta) V_0)}{V_9^2 + \beta V_{19}^2 - (1+\beta) V_0^2} \quad (2.64)$$

### 2.4.6 Global efficiency

This parameter compares the power the engine receives with the one fuel provides. So the definition can be established as follows:

$$\eta_0 = \frac{V_0 T}{\dot{m}_f L} = \frac{TSV_0}{fL} \quad (2.65)$$

Note that the obtention of the global efficiency can also be obtained by multiplying both previous efficiencies:

$$\eta_0 = \eta_{th} \cdot \eta_{prop} \quad (2.66)$$

Also, this magnitude can be related with the previous ones studied. For instance, from eq. 2.56 and combining it with 2.65:

$$TSFC = \frac{\dot{m}_f}{T} \quad \longrightarrow \quad \eta_0 = \frac{V_0}{TSFC \cdot L} \quad (2.67)$$

an expression combining efficiency and consumption can be obtained:

### 2.4.7 Parameters interaction

All parameters shown in 2.4 are not linearly independent, but there is a relation among them. By taking eqs. 2.54, 2.56 and 2.60, assuming no secondary flow:

$$\begin{aligned} TSFC &= \frac{\dot{m}_f}{T} \\ \eta_{th} &= \frac{V_9^2 - V_0^2}{2 f L} \\ TS &= V_9 - V_0 \end{aligned} \quad (2.68)$$

solving  $f$  in the two first:

$$\begin{aligned} f &= \frac{V_9^2 - V_0^2}{2 \eta_{th} L} \\ f &= TS \cdot TSFC \end{aligned} \quad (2.69)$$

equalling both expressions in 2.69:

$$\frac{V_9^2 - V_0^2}{2 \eta_{th} L} = TS \cdot TSFC \quad (2.70)$$

substituting the third equation of 2.68:

$$TSFC = \frac{V_9 + V_0}{2 \eta_{th} L} = \frac{TS + 2 V_0}{2 \eta_{th} L} \quad (2.71)$$

So, analysing eq. 2.71, two conclusions can be obtained:

- Specific thrust and fuel consumption have a direct relation so, when one increases, also the other, and viceversa. Provided that both an increase of the first one and a decrease of the second one are desired, a trade-off is established. This fact will be later discussed .
- An increase in the thermal efficiency allows better values for both thrust and consumption. Thus, a way to improve engine performance is to perform better values for  $\eta_{th}$ .

### 2.4.8 Engine weight

Apart from the variables presented before, the evaluation of the engine weight must also be considered. This is a key parameter during the design of a power plant, provided that it is incorporated in a flying vehicle. According to this reasonment, although a very powerful, low-consumption system might be built, if it is too heavy the aerodynamic effort to cover the increase in weight difficulties the design of the rest of the aircraft, disabling, in the worst scenario, the vehicle to fly.

This parameter is then used to compare engines. However, a more specific analysis should be carried out. Let us propose the following case: two engines, A and B, such that weight of A is a little bit greater than B, but its specific thrust is quite higher. Then, although it is heavier, its better performance might be preferred and then it would be installed. For this reason, rather than total engine weight, a more intensive variable should be used to get a more realistic idea of the plant performance.

Hence, the weight is compared with the specific thrust of the whole, (i.e. by a ratio among them), giving the weight-to-thrust ratio, WT, which is used in practice as the performance parameter related to the aircraft engine.

### Torenbeek's approach

A method to estimate the weight-to-thrust ratio was developed by Torenbeek[8] in 1975. Following a physics-based approach, the engine weight was modeled as a combination of the gas generator weight and the weight of the propulsive device[9]. A correlation, shown in eq. 2.72, was produced, assuming the gas generator weight is linearly linked to its mass flow, whereas the propulsive weight is proportional to the fan thrust at takeoff[9].

$$WT = C_1 W_{gg} + C_2 FN_f \quad (2.72)$$

where  $W_{gg}$  is the gas generator massflow and  $FN_f$  is the fan thrust.

On 2.72, constants  $C_1$  and  $C_2$  were obtained by correlating real data. After that, the final form of Torenbeek's correlation (eq. 2.73) is obtained.

$$WT_{to} = \frac{10 \cdot OPR^{1/4}}{TS_{to} \cdot (1 + BPR)} + 0.12 \cdot \left( 1 - \frac{1}{\sqrt{1 + 0.75 \cdot BPR}} \right) \quad (2.73)$$

where the subindex *to* refers to take-off conditions, and  $OPR$  is the overall pressure ratio, that is,  $OPR = \frac{p_{3t}}{p_0} = \beta_f \cdot \beta_c$ . Imperial units must be used, and the method cannot be used for high bypass ratio engines[8].

### Jenkinson approach

On the other hand, Jenkinson et al. developed[10], in 1999, a method based in the bypass ratio (eq. 2.74). Not only existing, but also projected high bypass ratio engine data were used to create the correlation[9].

$$WT_{to} = 8.7 + 1.14 BPR \quad (2.74)$$

A direct linear dependence with bypass ratio is observed. This approach is based on the supposal that fan weight, which is directly related to its size, increases more than the reduction of engine core weight, and thus total weight increases with higher by-pass ratio.

# Chapter 3

## Methodology

### 3.1 Introduction

Next, the method followed to estimate engine performance is explained, as well as the optimization and selection procedures conducted in ModeFrontier<sup>®</sup>.

### 3.2 Engine performance estimation

#### 3.2.1 Required information

Firstly, it is important to know which information concerning both engine and mission must be known. In particular, mission requirements are stated, as well as definition of both input and output variables in the code is performed. Moreover, other information concerning the Brayton cycle, but not treated neither as input nor output, is modeled.

#### Input parameters

Here, selection of the engine variables suitable to be modified in the optimization study is performed. Most representative parameters of an engine should be included, as well as any other variable whose modification seems to be essential for the search of an optimum state. Nonetheless, selection must be done carefully, since the more parameters are included in input, the more time the optimization algorithm requires for finding a solution.

Hence, the following parameters have been decided to work as input:

- Pressure ratio in the fan, noted in the analysis as  $\beta_f$ . Although it is not commonly included inside main engine information, its modification is easily reachable, so it has been included. The reason is that, if its influence in the optimum is proved, the former can be reached by an easy modify.
- Pressure ratio in the compressor,  $\beta_c$ . This is a key parameter in an engine. Again, a higher or lower value is got just by adding or removing compression stages. Current trend deals with performing greater and greater values for  $\beta_c$ . Thus, coherence in this practice wants to be found.
- Turbine inlet temperature,  $TIT$ . This parameter, that represents the maximum temperature found in the cycle and is hard to increase, is one of the most important variables in an engine. Companies use to hide this value in databases, since it marks the technology level of the enterprise (higher TITs means the company can develop materials which stand this temperature).

An increment of the thermal efficiency is got when rising the working temperature, reason by which a growing trend is got. However, the benefit in other performance parameters should be also proved. Note that this value equals to the variable  $T_{4t}$  shown in chapter 2.

- Bypass ratio, BPR. It shows how big is the fan compared with the core. By assembling a bigger or smaller fan, BPR can be modified, so studying its influence in engine performance has been considered interesting. Note that this parameter correspond to variable  $\beta$  in chapter 2.

### Output parameters

In this category all performance parameters should be included: the best engine is considered to have an optimum performance at all levels and fields. However, a greater number of variables to be optimized means exponential increase in the computational effort. For this reason, a selection among magnitudes studied in section 3.2 must be carried out.

In this project, the efficiency of the Brayton cycle concerning turbofan engines core has not been studied, but focus on the whole engine performance has been conducted. Then, the following variables have been chosen to perform the engine optimization study:

- Thrust specific fuel consumption, or TSFC. Fuel consumption has become the main performance parameter in commercial aviation, so it must be included in the study. Its minimization has become critical -and hard to achieve- for all manufacturing companies, and big efforts are put in this field.
- Specific thrust, TS. Thrust is the main performance parameter of any engine. For better cycle treatment, an intensive variable is used. As a last resort, this parameter resolves whether an engine is appropriate for an aircraft or not, depending on demanding thrust is accomplished with or not.
- Weight-to-thrust ratio, WTT. As commented before, engine weight is critical when flying the vehicle. Lower weight means more payload for an airline, or less consumption for the same mission. The inclusion of this magnitude in the study becomes a new point in the study of design optimization.

### Mission parameters

Now, external conditions must be set, that is, context on which the study aims to be carried out has to be stated. As commented before, this project is focused on commercial aviation only. Moreover, design conditions are considered. In a commercial flight, this point corresponds to the cruise phase, on which ambient conditions rarely change.

Hence, the optimization of the engine performance is studied for the flying -and unchanging- conditions shown in table 3.1

Mission parameters		
Name	Symbol	Value
Mach	$M [-]$	0.8
Altitude	$z [m]$	10000

Table 3.1: Mission parameters under which optimization study is performed.

As it can be observed, typical values for commercial routes have been chosen.

### Other parameters

Once selection of key and mission parameters, the rest of the variables needed for the obtention of the performance are considered as situational parameters. These magnitudes, the numerical value of which is also required to perform calculations, are not considered to directly influence in the output. Thus, fixed and reasonable values should be chosen. Numerical values for variables of this nature are presented in table 3.2.

Situation parameters					
Name	Value	Units	Name	Value	Units
Fluid constants (air)			Isentropic efficiencies		
$\gamma_{air}$	1.4	[-]	$\eta_d$	0.9	[-]
$\gamma_{gas}$	1.33	[-]	$\eta_f$	0.9	[-]
$R_{air}$	286.9	[J/(kg K)]	$\eta_c$	0.87	[-]
$R_{gas}$	286.9	[J/(kg K)]	$\eta_t$	0.98	[-]
Fluid constants (fuel)			$\eta_n$	0.98	[-]
$Q_f$	43.5	[MJ/kg]	Mechanical efficiencies		
Combustion efficiencies			$\eta_{mc}$	0.99	[-]
$\eta_{mf}$	0.99	[-]	$\eta_b$	0.95	[-]
$\eta_{mt}$	0.99	[-]	$\eta_{pb}$	0.95	[-]

Table 3.2: Other contextual parameters used in the study.

### 3.2.2 Implemented code

In order to calculate the Brayton cycle and then obtain the performance parameters, a code in Wolfram Mathematica<sup>®</sup> has been developed. This code, named *EngineOptimizationModel.m*, has been created as an internal library in the program. In this way, the whole process is saved as a function that can directly be used in future sheets. Moreover, storage of useless data is avoided.

Firstly, input data are imported. Variables present in the optimization are stored in a .txt file called *design\_parameters.txt*. Data are located in a column, and the order of the variables is the following: by-pass ratio, fan pressure ratio, compressor pressure ratio and turbine inlet temperature. An illustrative example of it is shown in fig. 3.1.

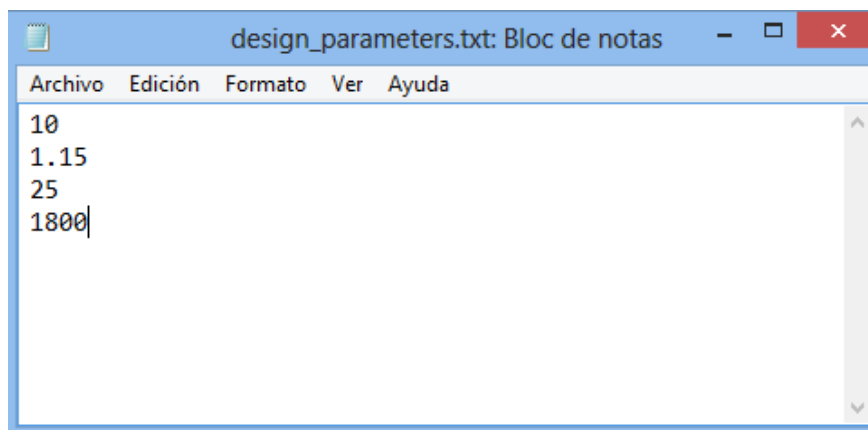


Figure 3.1: Example of a *design\_parameters.txt* file.

Then, these data are imported in Wolfram Mathematica<sup>®</sup> and stored separately. All these steps are written in a Wolfram Mathematica<sup>®</sup> module called *ImportMyData*.

Next, the rest of the working variables is loaded. Variables and values from tables 3.1 and 3.2 are written. This information is packaged in another module called *Datapackage*.

Furthermore, provided that the simulation is performed during cruise, and not at sea level conditions, an atmospheric model must be set. For this study, the International Standard Atmosphere, or ISA, has been used. This model, which has been built by data acquisition during several decades, models air as an ideal gas and considers a linear temperature decrease with altitude. Average values in intermediate latitudes are given[11] Air conditions regarding this model are shown in eqs. 3.1 to 3.3.

- Troposphere  $0 < z < 11000 \text{ m}$

$$\begin{aligned} T(z) &= T_0 - 6.5 \frac{z}{1000} \\ p(z) &= p_0 \left( 1 - 0.0065 \frac{z}{T_0} \right)^{5.2561} \\ \rho(z) &= \frac{p(z)}{RT(z)} \end{aligned} \quad (3.1)$$

with reference sea-level values  $T_0 = 288.15 \text{ K}$  and  $p_0 = 101325 \text{ Pa}$

- Tropopause  $11000 < z < 20000 \text{ m}$

$$\begin{aligned} T(z) &= T_{11} \\ p(z) &= p_{11} e^{-\frac{g}{RT_{11}}(z-11000)} \\ \rho(z) &= \frac{p(z)}{RT(z)} \end{aligned} \quad (3.2)$$

with reference values  $T_{11} = 216.65 \text{ K}$  and  $p_{11} = 22632 \text{ Pa}$

- Stratosphere  $20000 < z < 32000 \text{ m}$

$$\begin{aligned} T(z) &= T_{11} + 1.0 \frac{(z - 20000)}{1000} \\ p(z) &= 100 \left( \frac{44331.514 - z}{11880.516} \right)^{5.2561} \\ \rho(z) &= \frac{p(z)}{RT(z)} \end{aligned} \quad (3.3)$$

where SI units must be used.

Note that the model shows that temperature descends while going far from ground. Then, it remains constant in the tropopause, and a smooth increase is found above this layer.



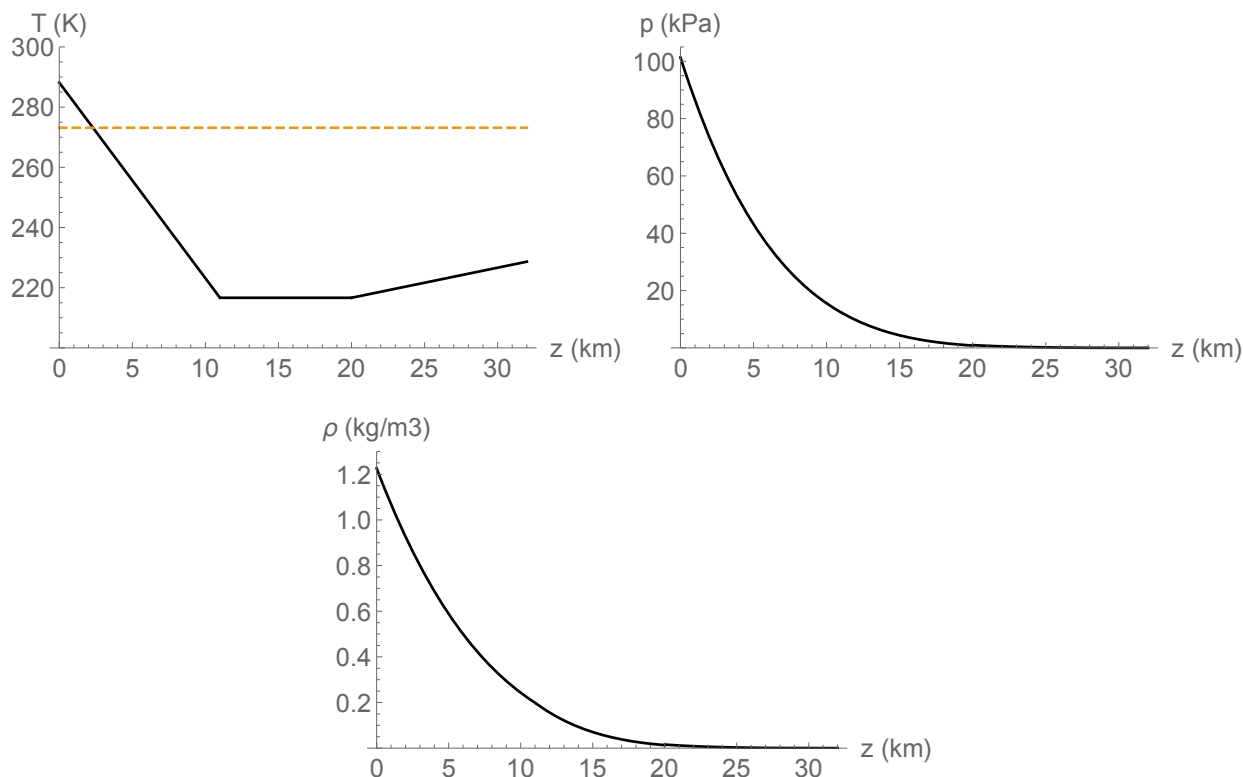


Figure 3.2: From left to right and top to bottom: air temperature, pressure and density according to ISA model.

Next, the cycle is solved. To do so, eqs. shown in sections 2.3.2 to 2.3.8 are used: intake, fan and main compression, combustion, turbine and nozzle expansion are applied to the primary flow, whereas only fan compression and nozzle expansion are simulated for the bypassed flow.

Then, engine performance can be obtained: eqs. from sec. 2.4 are used, and parameters are given.

### Weight model selection

Weight is also evaluated together with other performance magnitudes. However, as seen in 2.4.8, two different correlations can be used. A different range of applicability is noted, according to the authors[8],[10].

Then, a different correlation should be used depending on engine specifications. Particularly, the distinction is made in the value of the BPR: results for low bypass ratio engines seem closer to Torenbeek's approach, whereas high bypass ratio ones are better modeled by Jenkinson's.

For this reason, both correlations have been tested for real engine data, and trends of each one of them have been analysed.

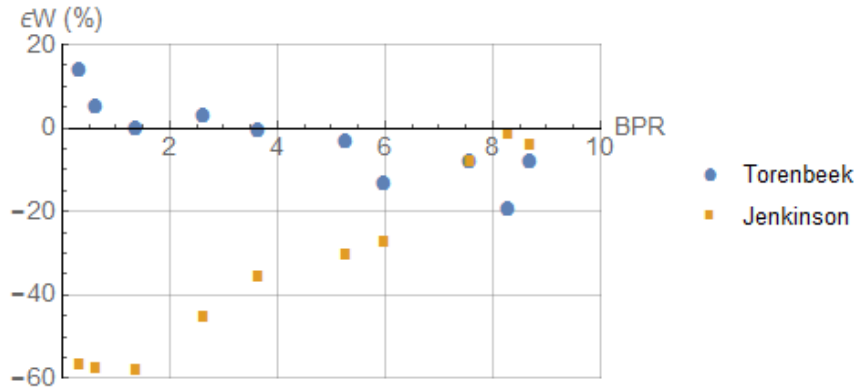


Figure 3.3: Relative error between real engine weight and correlations studied for according to BPR.

Two different trends can be observed: for low bypass ratio engines, Torenbeek’s correlation seems to offer better results; when BPR is higher, Jenkinson’s model performs a better approach. Thus, author’s notes regarding the range of applicability have been confirmed. Rather than checking specifications are right, an intermediate value on which separating the useage of both models had is performed. According to fig. 3.3, a threshold value equal to six has been stated. Hence, if the case planted has a bypass ratio lower than six, Torenbeek’s model will be used to estimate weight-to-thrust ratio in the engine performance, whereas if the value is greater than six, Jenkinson’s will be taken.

$$BPR_{th} = 6 \quad (3.4)$$

Note that in Torenbeek’s correlation sea-level specific thrust is required. Hence, the cycle has to be solved again, assuming  $z = 0$ , specific thrust under these conditions is calculated with eq. 2.54 and weight-to-thrust ratio is given.

### Removing inadequate cases

When BPR, pressure ratios and TIT are introduced in the input, a study of the multiple cases found must be done. The Brayton cycle exposed is limited to some proper combinations of the variables. Provided that some characteristics are fixed, the rest of the input parameters should be chosen such that a solution can be achieved. In other words, not any combination of the four inputs is appropriated to perform a valid solution of the cycle. For instance, if the temperature in the turbine entry is fixed to a low value, but a high compression is stated, no concordance in the results is reached, and solution tends to be “rare” (i.e. in the complex field).

Hence, unsolvable cases must be identified. To do so, a new variable is included in the output package. This variable checks if all the performance parameters calculated take reasonable values. If so, a flag is risen, otherwise, not ok signal is given. Particularly, all cases in which at least one of the performances is not a real and positive number -note that all variables taken in the study must take positive values-, a zero is output together with the results, and all parameters are symbolically changed to -1. This procedure is also helpful in the optimization algorithm. If the cycle has been solved properly, a number 1 is stated and no changes are done in the performances.

Finally, results are kept and exported in another .txt file, called *results.txt*. This file contains the performance parameters selected. The order is the following: thrust specific fuel consumption, specific thrust, weight-to-thrust ratio (calculated with the appropriate method) and the solution flag variable. Note that all variables are output in SI units.

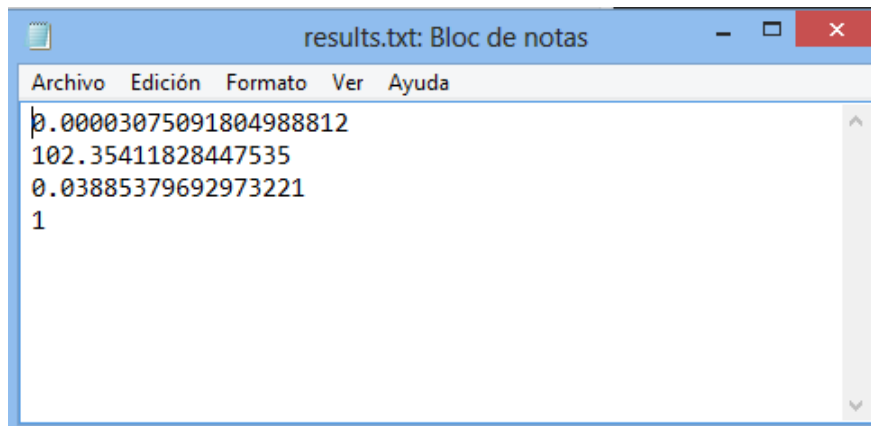


Figure 3.4: Example of a *results.txt* file.

Note that one only case must be inserted as input: if more case study is needed, the process must be repeated.

### Run file

Once the library is created, it is loaded and run in a Wolfram Mathematica<sup>®</sup> notebook, named *EngineOptimizationModel.nb*. In it, file containing design parameters is loaded, and results are written in the specified folder.

## 3.3 Optimization procedure

Once the engine performance is calculated and organised, the research of an optimum point that satisfies all requirements in the best way is conducted.

To do so, an optimization software has been developed in ModeFrontier<sup>®</sup>. In this file, the Wolfram Mathematica<sup>®</sup> notebook is interacting with this program, working schema is set, cases are repeated several times, and results are obtained.

### 3.3.1 Working frame

First, a macro on the frame is created. In this sheet, named *EngineOptimizationModel.prj*, all variables involved (i.e. inputs, outputs, external files used, optimization algorithm, etc) are connected. It allows to perform calculations in the software, so that results can be obtained.

The working sheet used in this project is shown in fig. 3.5.

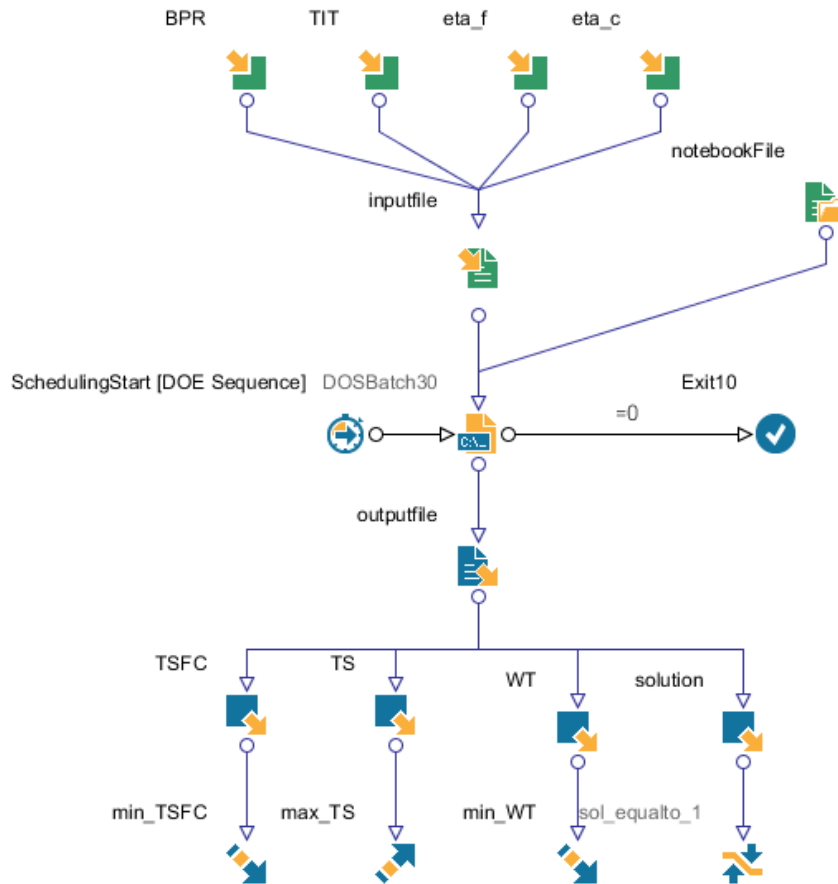


Figure 3.5: Workflow used for the study of the optimum design point.

Next, the role of each component in the workflow is explained.

Firstly, input and output variables must be defined. In this case, the pack of all design parameters set the input, according to explanation in 3.2.1. In the same way, all performance parameters form the outputs, as seen in 3.2.1. Note that another output called “*solution*” has been added. This binary variable, which is also contained in the *results.txt* file, shows whether the cycle has been properly solved or not.

Together with any output, a target is defined. This procedure is compulsory, given the mission of the software, which is not other than optimise variables. Hence, desired trends are specified: both fuel consumption and weight-to-thrust ratio are set to reach the minimum allowable, whereas both specific thrust aims to be maximum. Note also that a harder restriction is imposed to the *solution* output: equality to the unit must be achieved. This is a way to ensure that results obtained are trustful, that is, unsolved cases are removed from the study.

Both input and output variables are connected to its respective file. These files, named as *inputfile* and *outputfile* in the sheet, represent the connection between programmes. In them, numerical values inserted in the *design\_parameters.txt* file are referred to each variable in the workflow. The same link is performed for the outputs.

Next, the file on which calculations are performed is included together with the inputs. This file is the *EngineOptimizationModel.nb*, presented in 3.2.2.

Finally, both halves are linked by the core of the whole. This part is the one who runs calculations in modeFrontier<sup>®</sup>. The usage of an external software, in this case Wolfram Mathematica<sup>®</sup> is specified, and the notebook that must be run is set. To do so, the path to this file is written, in

cmd nomenclature.

### 3.3.2 Design of experiments

Note that a component has been omitted in the previous section. This node, located in the left part of the batch, refers to the design of experiments, or DOE, configuration. The design of experiments is the part in which all cases, or experiments, are launched. An experiment is created just by a combination of inputs.

Before the experiments are created, limits in the values should be established. In this case, lower limits are set to the minimum values reachable by any input parameter, given its nature. For instance, bypass ratio cannot take negative values, being zero the minimum case (note that in this case the engine would be a turbojet), whereas pressure ratios must be greater or equal to 1. Upper limits, on the other hand, do not have a mathematical limit, so current technology has been used as a reference, except for bypass ratios, whose optimum conditions tend to appear for very high values[4]. Both lower and upper limits used in this project are shown in table 3.3.

Limits configuration		
Name	Lower	Upper
BPR	0	10
$\beta_f$	1	2.5
$\beta_c$	1	50
TIT	800 K	2500 K

Table 3.3: Lower and upper limits set for design parameters.

Once the space on which experiments are enclosed, multiple distributions can be used. There are multiple ways to create an experiments set, and the usage of one or another depends on the target the analysis has. In this study, particularly, two DOE configurations have been used:

- Full factorial: this distribution corresponds to a uniform spread in the specified domain. In other words, variables are equispaced between the limits. A regular mesh is formed in the  $n$ -dimensional space, being  $n$  the number of inputs. The length of each side is equal to the number of different values that has been specified for each variable.

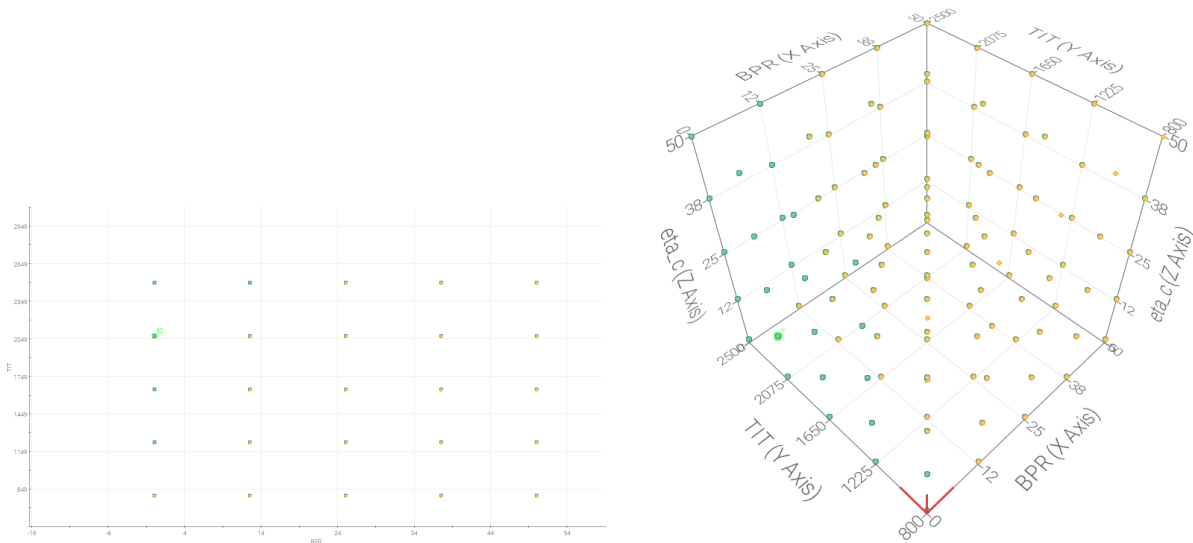


Figure 3.6: Example of a 2D (left) and 3D (right) full factorial DOE.

- **SOBOL**: this algorithm performs a pseudo-random distribution of data, and experiments are uniformly distributed in the design space. In this case, the density is calculated in such a way that all parts of the domain are properly represented and modeled. As the full factorial model, n-dimensional designs can be performed.

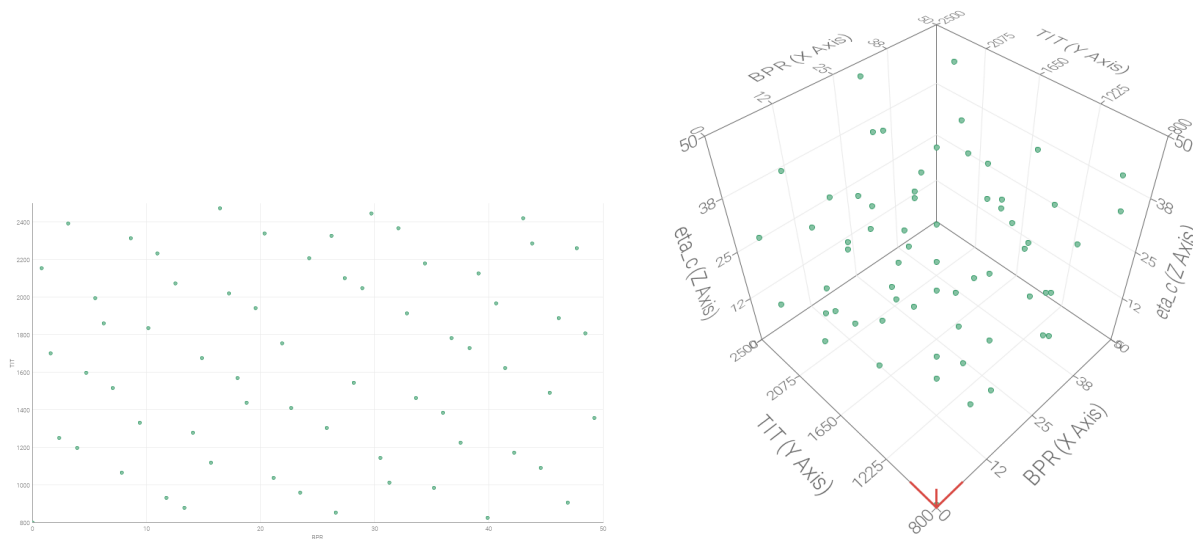


Figure 3.7: Example of a 2D (left) and 3D (right) sobol DOE.

Each experiment created in the DOE will be run applying code found in the notebook and results will be stored for later postprocess.

### 3.3.3 Sensitivity analysis

Before running the macro, a preliminary study should be conducted: the sensitivity of the output variables according to the inputs should be known. The aim of this study is to know the influence

each variable, either incoming or outgoing, has into the others. If no correlation between two variables is observed, the input one can be removed from the latter optimization algorithm, or at least relaxed, provided that no changes will appear whether this variable is included in the analysis or not. Hence, computational effort is saved. The greater the number of variables are initially involved in the study, the more important this first analysis is, since uncorrelation is more likely to appear and the number of cases to be simulated becomes factorially less.

This analysis has been performed as follows: first, a full factorial DOE is created for the domain provided in table 3.3. Since cases belonging to the whole range want to be simulated, this algorithm becomes the best choice to do that. Hence, tendencies and relations are given considering all the participants, although the range of interest might become quite smaller in the optimization point.

The aim of this analysis is to quantify the variation in the performances when one of the design parameters is changed. To do so, several magnitudes can be used. In particular for this study, the following magnitudes have been used for studying the sensitivity:

- Correlation matrix: this matrix is useful for verifying whether there is a linear -positive or negative- relation between variables. The correlation ranking shows the most relevant connections. High values (i.e. greater than 0.7) indicate real influence only. Moreover, a scatter matrix indicating scatters can be plotted too.

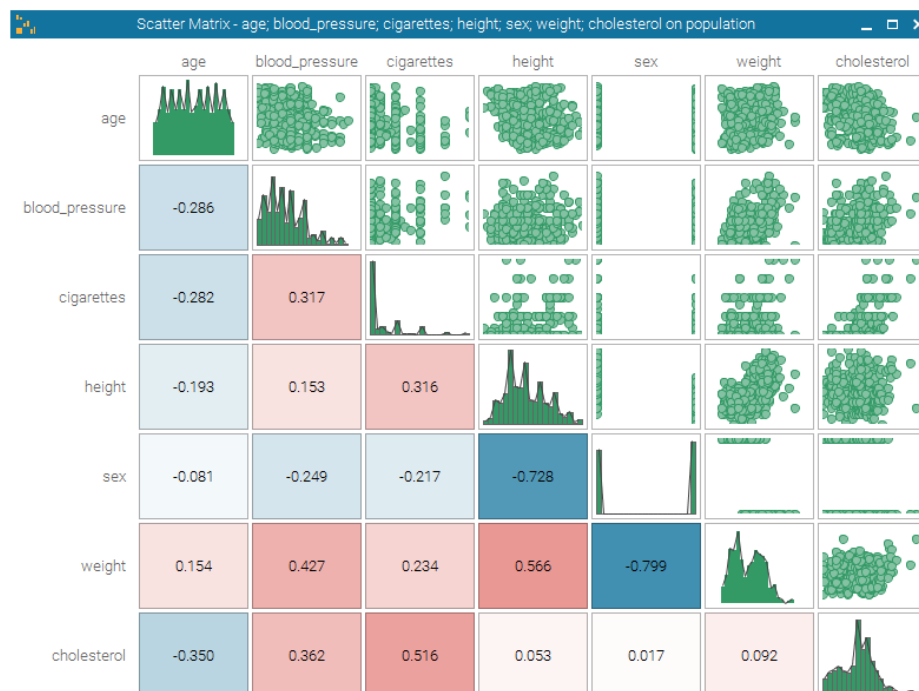


Figure 3.8: Example of linear relations between variables. Correlation matrix is plotted in the lower left corner and the scatter matrix can be found in the upper right one.

- Overall student analysis: the t-Student test is useful for identifying the most important causes of an undesired effect. It may therefore enable to make a correct diagnosis for a new subject just by looking at a few parameters instead of the whole set.

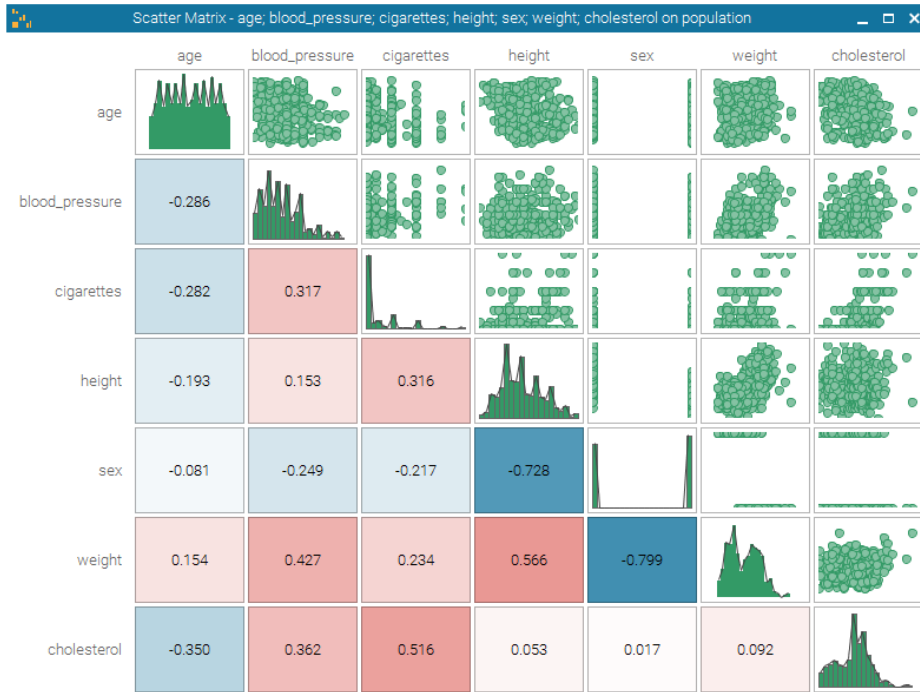


Figure 3.9: Example of pie chart based on a t-Student analysis.

- Parallel coordinates: this is the best way for data interpretation when the number of variables involved is high. In this chart, each parameter is represented in a vertical bar, and each value it takes means a cut with the bar. Then, each experiment is represented as a line path passing through all columns, where crossings show numerical values of the parameter. In figure 3.10 a graphical representation is shown for better knowledge.

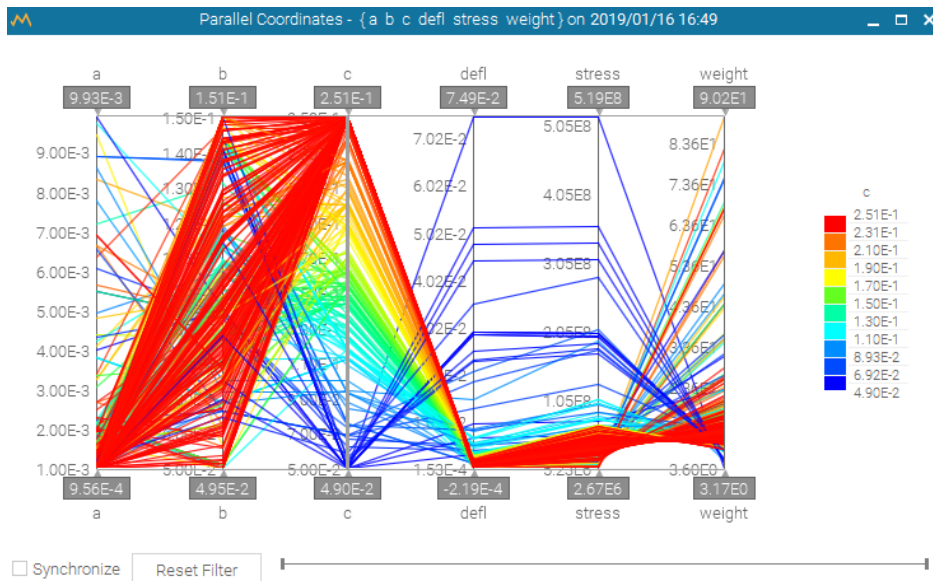


Figure 3.10: Example of a parallel coordinates chart.

Another advantage this chart offers is data filtering, both graphically and in table format. So,



it is a very good tool in optimization search, however, it is not the best plot for observing and analysing sensitivity.

- Furthermore, the program itself offers the possibility to perform an overall sensitivity analysis. The influence of all parameters specified in the one selected is given in a bar chart, as well as the cumulative effect. The number of variables, by order of importance, or the top cumulative effect considered can be configured. Although it is the analysis the program recommends, a good practice is to carry out and study other chart for a wider knowledge of the phenomenon.

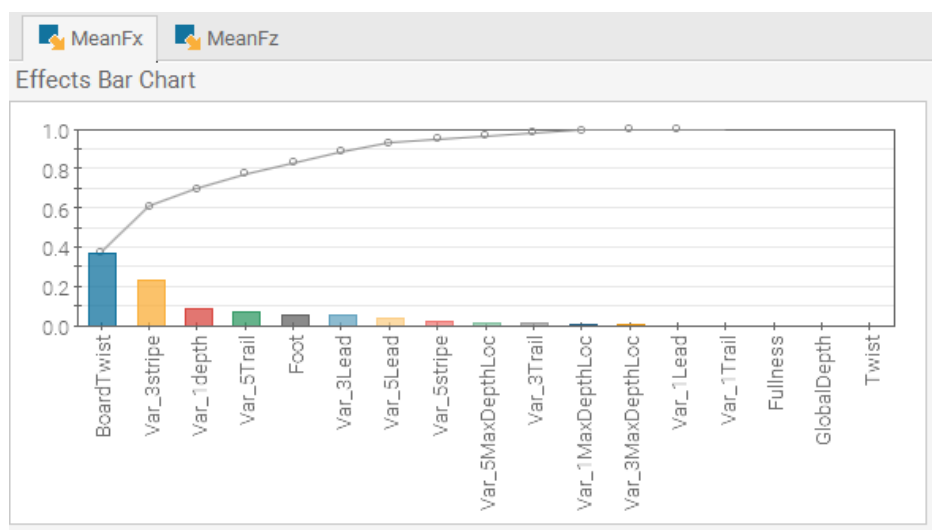


Figure 3.11: Example of a sensitivity chart.

### 3.3.4 Optimization algorithm configuration

Once experiments to be run are designed, next step deals with the research of an optimum point inside the experiment net created. To do so, an optimization algorithm must be selected. This code provides the input combination that best fits with requirements stated, either one of existing DOE's itself or a new experiment created by the system.

This study has been conducted by using the so-called MOGA II algorithm. This algorithm, whose acronyms mean Multi-Objective Generic Algorithm, uses a smart multisearch elitism for robustness and directional crossover for fast Pareto convergence[12].

The workflow of the MOGA method is explained as follows:

- The initial population is selected. In this case, this population corresponds to the DOE set defined.
- Next, the algorithm creates a new population, which is created via cross-over and mutation:
  - Cross-over combines two parents to generate a new chromosome. The idea behind is that the new chromosome may be better than both of the parents provided that it takes the best characteristics of both only.

There are several ways to generate children. The most popular ones are performing a linear combination among two parents applying a porcentual parameter, or a uniform combination in which the operator itself decides which parent is contributing each gene in the chromosomes.

Directional crossover is also used. In this technique, the algorithm assumes that a *direction of improvement* can be detected by comparing the fitness values of two reference individuals[12]. This direction is evaluated by comparing the fitness of the individual  $i$  of generation  $t$  with the one of his parents. The new individual is then created by moving in a randomly weighted direction that lies within the ones individuated by the given individual and his parents[12].

- Mutation alters one (or more) gene values from its initial state. The aim is the obtention of a completely new genoma, that may arrive to a better solution.

For continuous parameters, a polynomial mutation operator is applied to implement mutation, whereas for discrete values cross-over is performed for each gene with a probability of 0.5.

- After the first iteration, each population is run a number of times that must be specified in the method.
- Design points are now updated in the new population.
- Finally, converge is validated. A model is converged when the maximum allowable pareto percentage or the convergence stability percentage are reached[13]. On the other hand, if optimization is not converged, stopping criteria are searched. In the case this case is neither reached, the algorithm returns to the new population creation step.

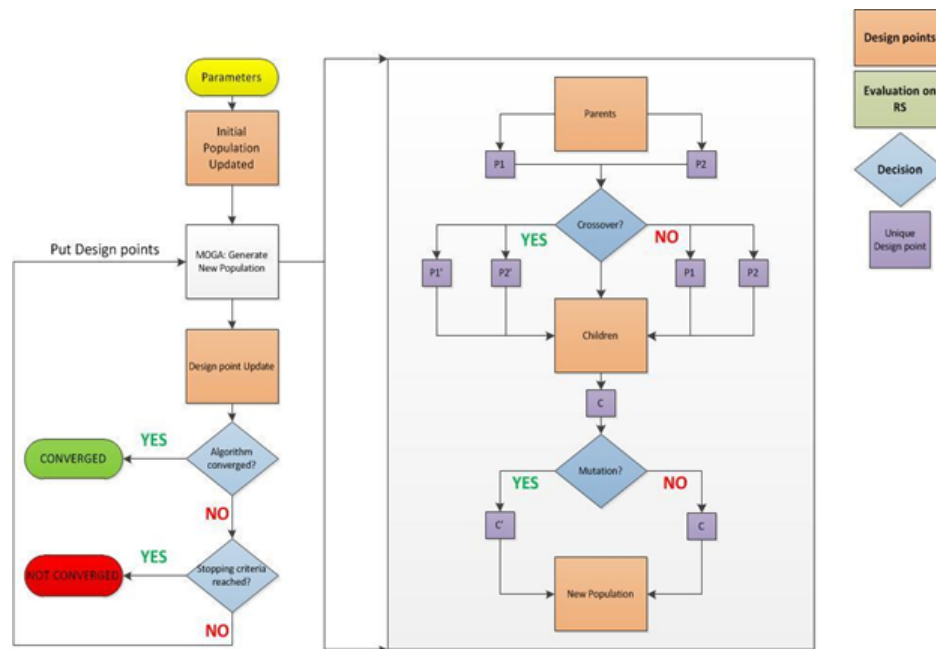


Figure 3.12: MOGA-II workflow.

The selection schema in MOGA-II uses to be a local tournament with random steps in a toroidal grid[12]: an individual subject is chosen as the starting point, and candidates are chosen by following a random walk, unique for each candidate. Once the set is generated, the best member is chosen.

This code support all types of input parameters. Moreover, it also ensures that feasible solutions are always ranked higher than the unfeasible ones.

The first Pareto front solutions are stored in a separate sample set internally and are different from the evolving sample set. In this way, minimal disruption of previous Pareto front patterns is ensured.

The main features of this configuration, according with ModeFrontier<sup>®</sup>, are the following:

- It provides geographical selection and directional cross-over.
- The implement of elitism for multi-objective search.
- It handles constraints by applying the objective function penalization.
- It enables generational or steady-state evolution.
- It enables concurrent evaluation of independent individuals.



# Chapter 4

## Results

Throughout this chapter, results obtained after the implementation of the methodology described in the previous chapter are presented.

### 4.1 Sensitivity between input and output variables

In this section the sensitivity analysis explained in sec. 3.3.3 is presented. Full factorial DOE has been run and no optimization algorithm has been used. Results obtained have been filtered and unfeasible cases (those ones which do not accomplish with the *solution* output requirement) have been removed.

First, the correlation matrix is presented in fig. 4.1. In it, Pearson correlation coefficient, usually noted by  $R^2$ , is shown for each couple of variables.

Note that turbine inlet temperature has not been considered as a variable in this study, but fixed to a value of 1600 K. The aim of this removal is the obtention of reliable results, provided that the TIT is nowadays limited to an upper value.

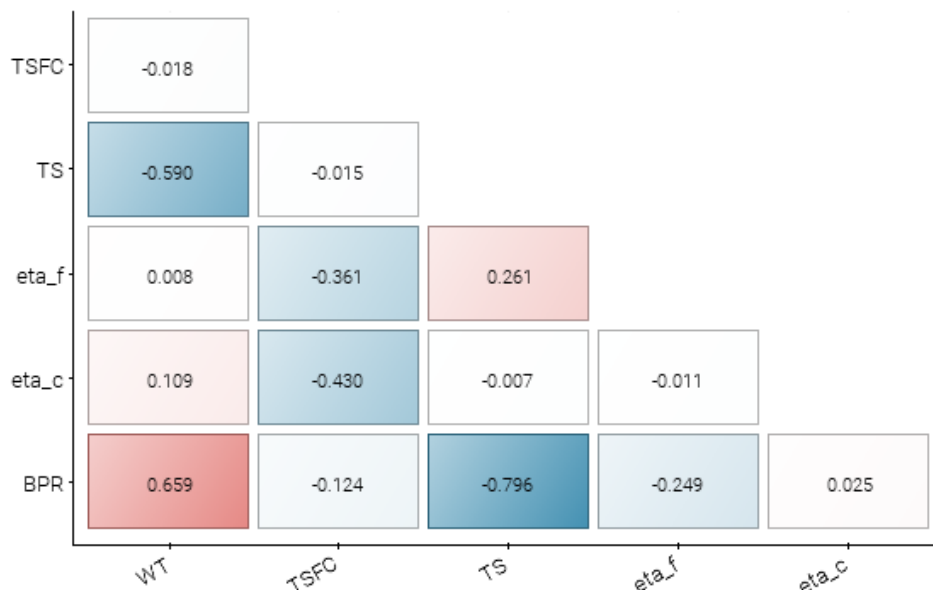


Figure 4.1: Correlation matrix involving design and performance parameters.

ERRATA SHEET: *eta* labels appearing in all plots shown in this section correspond to *beta*.

The strongest relation seems to be the one existing between bypass ratio and specific thrust. According to eq. 2.54, higher BPRs lead to thrust increase. However, since specific conditions refer thrust per unit of total airflow, which also increases with BPR, the trend is not clear.  $\beta$  has more influence in the denominator, provided that is the only term appearing on it, and, as a result, the relation takes an inverse nature.

The presence of the fan, that is, BPR, is also highly modifying engine weight, as should be supposed. Moreover, the influence on fuel consumption should exist, but no appreciable  $R^2$  is got. To perform a wider analysis, the scatter plot among these two parameters is graphed and shown in fig. 4.2.

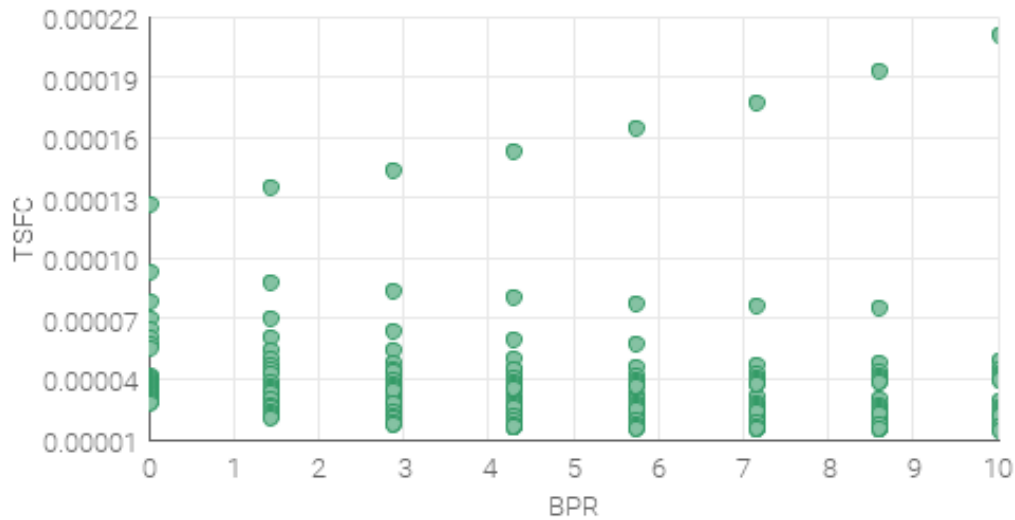


Figure 4.2: Scatter plot between bypass ratio and fuel consumption. TSFC is represented in SI units.

In fig. 4.2, lower consumption can be observed for increasing BPR, except for one family of DOE's. This is a particular casuistic where no compression at all is performed to the flow, that is,  $\beta_f = \beta_c = 1$ . This trend, that does not correspond to realistic situations, modifies the overall behaviour between the variables. Hence, neglecting this family, it can be stated that BPR leads to a fuel consumption decrease, as expected.

Returning to fig. 4.1, pressure ratios in both fan and compressor seem to have an influence in fuel consumption only. In fact, the higher air compression is, the lower fuel-to-air ratio is, resulting on a TSFC decrease.

Specific thrust and weight, although also affected by pressure ratios, are more dominated by BPR, and hence no remarkable coefficients are observed.

Another way to study variables interaction is applying the overall t-student analysis. In fig. 4.3, results for this analysis are shown.

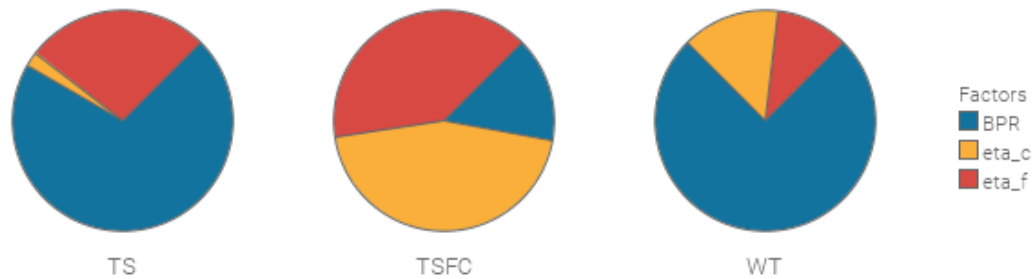


Figure 4.3: Overall t-student analysis of the study conducted.

Several conclusions can be extracted from this plot: firstly, specific thrust is dominated by by-pass ratio, which is in accordance with eq. 2.54. Second order effects are led by fan pressure ratio, whereas influence of compression in engine core is negligible. In summary, secondary flow domains engine performance in terms of specific thrust.

Regarding fuel consumption, all parameters seem to have an influence: although BPR is appearing as the less influencing variable, for real situations this relation is higher, as commented before. This equivalence in sensitivities relies on the fact that consumption is affected by many parameters, such as fuel-to-air ratio, bypass ratio, and jet exhaust speed, among others.

Finally, engine weight is mainly affected by bypass ratio implemented in the engine. The higher the BPR is, the higher and the heavier the fan is. Also, when adding compression stages, compressors become longer and hence heavier. Nonetheless, fan used to bypass airflow is the most affecting component on total engine weight.

As a conclusion, it can be stated that all input parameters considered for this study have an influence on outputs, so all of them should be included in the optimization study, the results of which are explained along the next section.

## 4.2 Selection of the optimum

To select an optimum design point, several DOE's have been launched, applying a MOGA-II optimization algorithm. A thousand simulations have been run, and results obtained can be observed below. Fig. 4.4 shows all (three) performance parameters obtained for each simulation. Both specific thrust and fuel consumption correspond to X and Y-axis, respectively, whereas engine weight has been plotted by using a colorbar. This is a 3-dimensional representation published in a 2D plot.

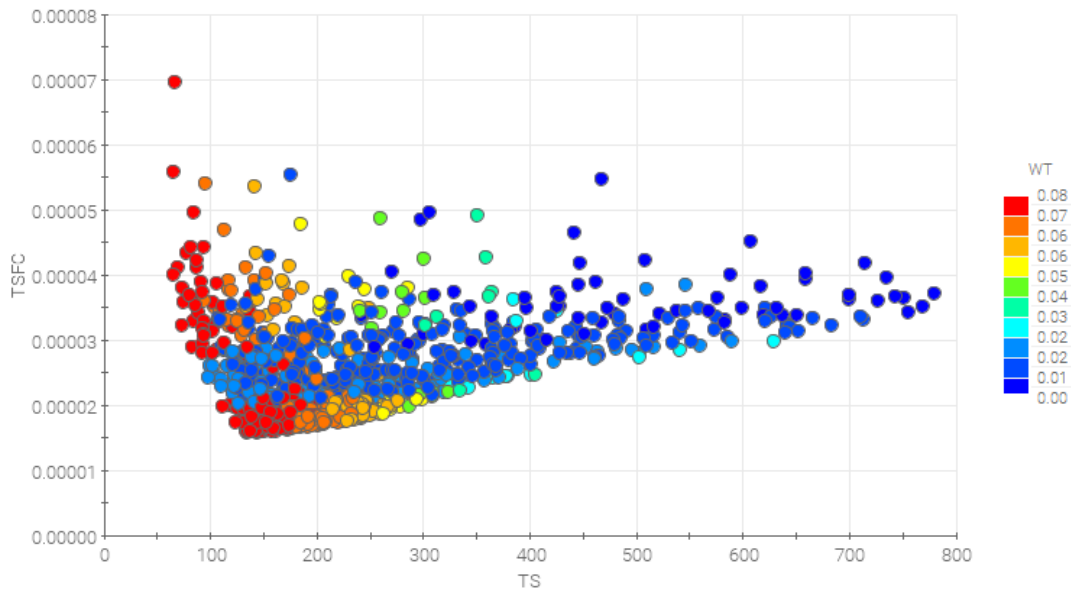


Figure 4.4: Engine performance according to design parameters stated and optimization algorithm used. All units correspond to SI.

Attending to thrust and consumption only, a Pareto front can be observed: less-consuming configurations provide very low values of thrust, whereas most powerful engines would consume high quantities of fuel. In other words, a wall or front is appearing, since best requirements according to both parameters (right lower corner in the graph) cannot be obtained. Hence, a trade-off must be established and a point that accomplishes with all requirements (as long as possible) should be chosen. Note that this Pareto front is mathematically represented by eq. 2.71.

In fig. 4.5, data are filtered in order to get the Pareto front. In this case, filtering has been applied to the whole study, that is, including engine weight in the front.

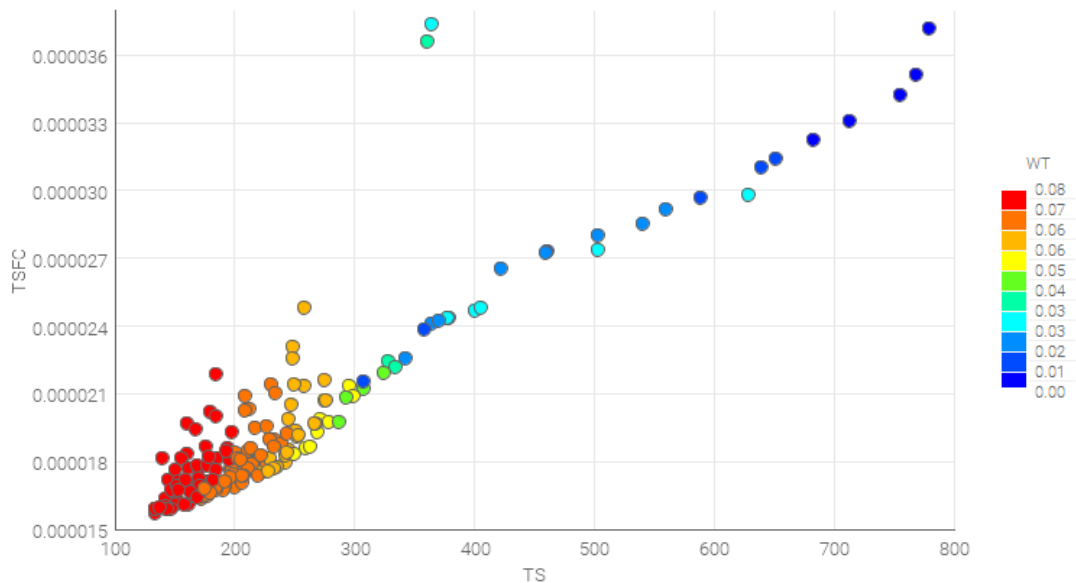


Figure 4.5: Pareto front of the engine performance. All units correspond to SI.



The 2-dimensional front concerning thrust and consumption can be observed. Since weight is also present in the study, the front includes some other points, even far from the wall, which correspond to lightest experiments simulated.

In this point, a decision must be taken by observing fig. 4.5. Trade-off between several performances should be established, but other decisions can be taken depending on the mission requirements. Below, some deciding criteria according to different mission requirements are presented.

#### **Solution A - minimum fuel consumption**

Fuel consumed by the engine is one of the main expenses in airlines. Because of this, lowest fuel consumption may be interesting from an economical point of view. As it can be observed, lowest consumptions are inherently linked to low specific thrust. Nonetheless, this issue may not suppose a problem as far as thrust demanded by the aircraft is as low. Another way to increase thrust is performing a bigger air intake, provided that thrust analysed here is referred to unit of massflow. Besides, weight increases for low-consuming solutions, as the model shows.

Hence, this solution may be adopted for small aircraft, whose demand in thrust is not high at all, or those ones with high aspect ratios, allowing enough lift to compensate weight increase. Nonetheless, the reduction in fuel cost and increase in engine development cost (due to weight increase) leads to a balance whose benefit from an economical point of view should be checked.

#### **Solution B - maximum thrust available**

In the other hand, mission requirements may set high aircraft thrust. If so, one point on the very right of fig. 4.5 should be selected. This selection leads to a very high fuel consumption, nonetheless, engine weight in this configuration is also very low. This configuration may be suitable for military applications, on which thrust available during mission domains against fuel consumed. The lightness of the engine for this solution contributes to the benefits of the choice, since a lighter aircraft increases its manoeuvrability, which is crucial in military applications.

#### **Solution C - lightest configuration**

Performing a very light engine may contribute to lift, and hence drag requirements. This solution may be interesting for some delta airplanes flying at transonic or supersonic conditions, where aspect ratio and wing surface are low, and drag is inevitably increasing because of high speed.

#### **Solution D - Full trade-off**

In real situations, however, these extremes are not usually taken, since harm in the non optimised variable(s) does not compensate benefits performed. For this reason, a trade-off must be established. The best practice is to trade all variables involved in the study: a configuration that provides acceptable values -although not the best achievable ones- should be found and selected as the mission point.

To do so, the three extreme cases presented above are taken, and numerical minimum/maximums are evaluated. Then, the delay in performance parameters referred to local optimums are calculated for each configuration in the Pareto front. The one giving the lowest maximum deviation for all variables is selected as the best 3D tradeoff solution.

#### **Solution E - Two dimensional tradeoff**

If weight is not considered in the analysis, the classical Pareto front appears, and the solution adopted may be different from the previous case. In this situation, the same procedure is applied,

but to consumption and thrust only.

Next, all solutions proposed are presented individually and inside the Pareto front in fig. 4.6

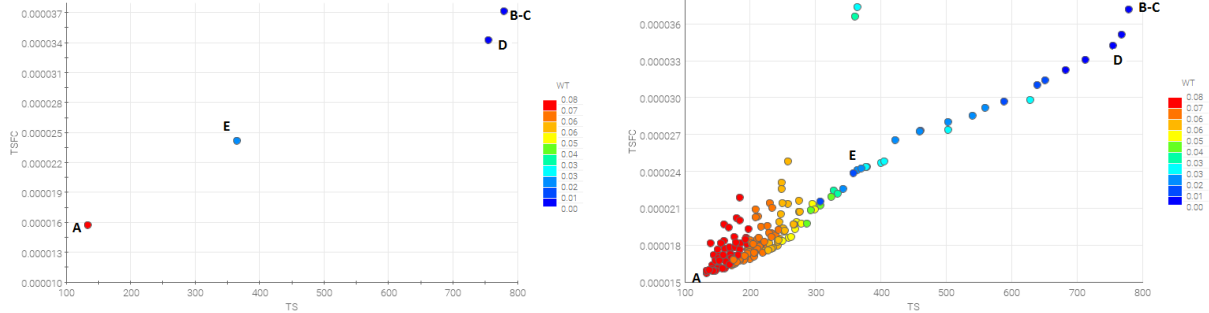


Figure 4.6: Solutions presented in the bubble chart (left) and together with whole Pareto front (right).

Note that both most powerful and lightest solution coincide.

#### 4.2.1 Summary and comparison of solutions presented

In this section, a summary of all configurations proposed for different optimizations are shown in table 4.1, and the differences in the Brayton cycle among them are pictured and commented.

Possibilities of performance optimization						
Solution	BPR	$\beta_f$	$\beta_c$	TSFC [N/(kg s)]	TS [m/s]	WTT
A	9.41	1.69	46.75	$1.57 \cdot 10^{-5}$	134.01	0.077
B-C	0.05	1.53	13.20	$3.72 \cdot 10^{-5}$	779.30	$3.96 \cdot 10^{-3}$
D	0.02	1.61	25.60	$3.42 \cdot 10^{-5}$	755.44	$6.92 \cdot 10^{-3}$
E	1.31	2.20	43.78	$2.41 \cdot 10^{-5}$	364.82	0.0025

Table 4.1: Key parameters of all solutions proposed as optimum configurations.

The less consuming solution is characterised by high both bypass ratio and pressure ratio in the compressor. To understand this behaviour eqs. 2.22 and eq. 2.54 must be analysed: fuel-to-air ratio is dominated by the remainder  $T_{4t} - T_{3t}$ , whereas specific thrust is highly depending on  $\beta$  and exhaust velocities. When increasing pressure ratio in the compressor, jet speed in both flows increases, as it can be seen in fig. 4.7. This would help in the consumption increase. However, at the same time, temperature difference is lower, resulting on a lower fuel-air ratio. Since this last trend domains, high flow compressions are required.

Moreover, high bypass ratio leads to a decrease in specific thrust, provided that denominator in eq. 2.54 is leading.

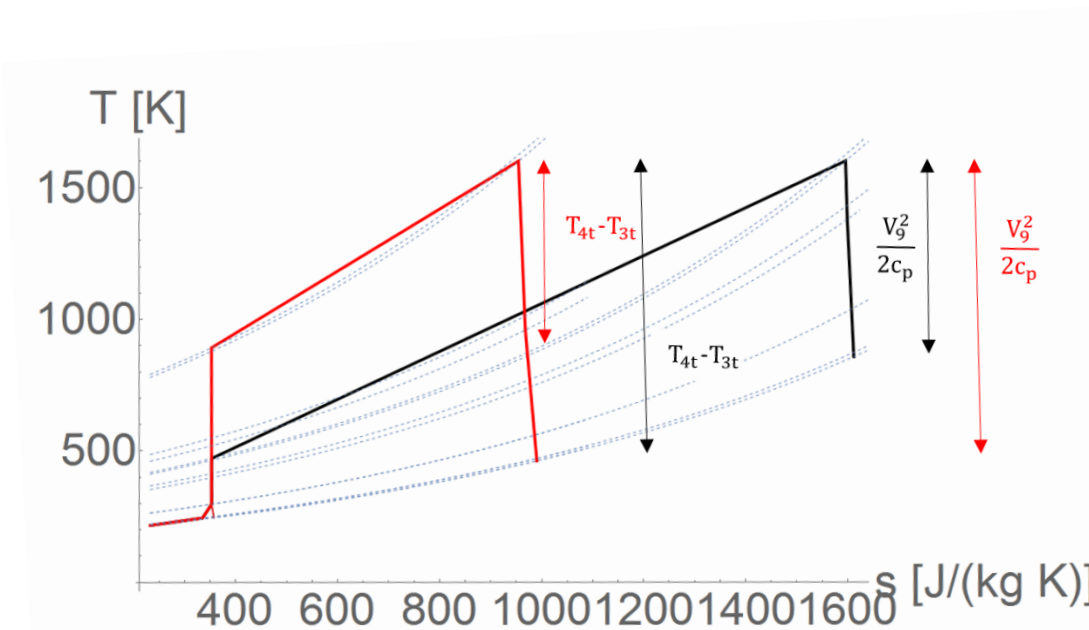


Figure 4.7: Brayton cycle comparing a low (black) and high (red) OPR engine.

Regarding highest thrust configuration, a very low BPR is needed according to eq. 2.54 knowing the denominator rules. This configuration, in fact, could correspond to a turbojet engine, instead of a turbofan, given the very low (almost negligible) value of  $\beta$ . Nonetheless, this model consumes a lot. This fact led to the translation to the use of turbofan engines, that allowed an important fuel consumption reduction.

Tradeoff solutions provide intermediate values for pressure ratios: according to Torenbeek's equation (2.73), low compressions must be conducted; however, this procedure leads to lower jet exhaust velocities, which reduce specific thrust.

Finally, when weight is not considered (solution E), the intermediate value between both thrust and consumption is got, as table 4.1 shows.

Next, relative deviations with respect to the optimums are presented in table 4.2. On it, the negative aspects of each solution adopted can be observed better.

Relative deviation between solutions			
Solution	TSFC dev.	TS dev.	WTT dev.
A	—	−82.8 %	1863.1 %
B-C	136.2 %	—	—
D	117.5 %	−3.1 %	74.7 %
E	53.3 %	−53.2 %	528.2 %

Table 4.2: Deviation in performance parameters with respect to local optimums.

The lowest consumption approach gives a disproportionately high weight, resulting on an engine almost 20 times heavier than the lightest option. Moreover, specific thrust is reduced by an 80%. These disadvantages should be considered if a very low consuming configuration is aimed, thrust requirements must be accomplished, and increase in weight should be considered in the aircraft aerodynamics, to ensure if the airplane is able to fly.

Most powerful and lightest configuration consumes more than the double of fuel than the optimum case. Nevertheless, two of the three requirements considered for this study are optimised.

Finally, tradeoff solution D reduces consumption in 17 percentual points, without losing thrust but increasing weight-to-thrust ratio by a 75%. A similar approach can be established to solution E, where consumption is even more reduced but weight is four times higher.

Note that, although high deviations may be observed, values are related to the very optimums, without considering how do the rvariables change. In other words, local optimums, though reachable theoretically, are never implemented due to the bad behaviour concerning other variables. Hence, comparisons shown in table 4.2 do not compare feasible and current cases.

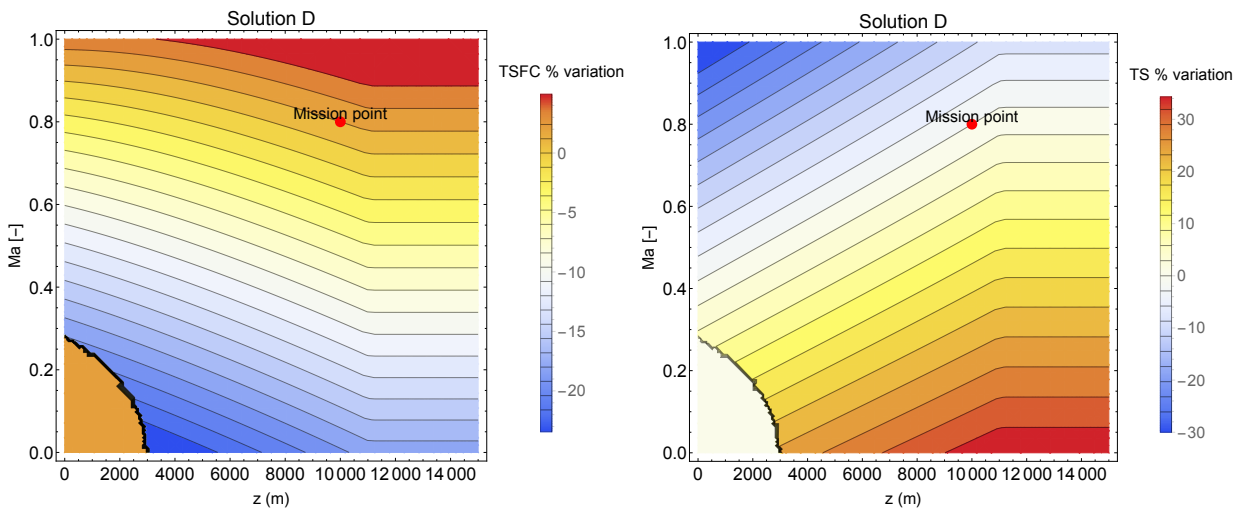
### 4.3 Influence of other parameters

Next, the influence of other internal and external parameters, that have remained constant during the research of the optimum, is studied.

#### 4.3.1 Mission parameters

First, mission parameters, (i.e. flight Mach number and altitude) are modified in order to evaluate the change produced in the performance. Different points have been studied, according to 4.2, and results are presented in a contour plot in which the x and y axis correspond to the mission variables and contours show the increase or decrease in the performance.

First, the most likely solution, that is, the 3D tradeoff os presented in fig. 4.8.



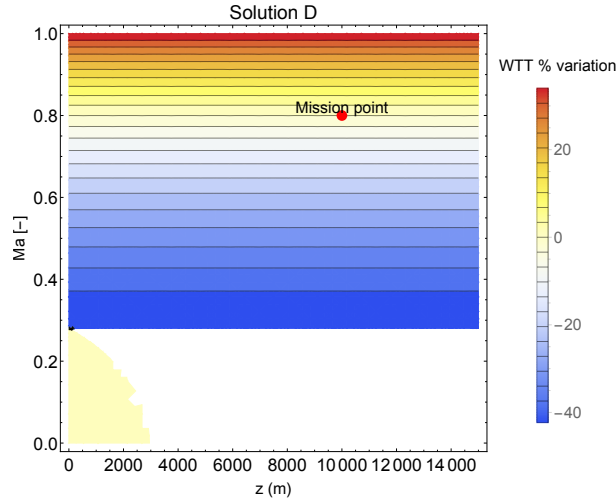


Figure 4.8: From left to right and top to bottom: engine performance variation as a function of mission parameters for configuration solution D.

According to fig. 4.8, altitude has a positive effect on specific thrust: when cruise altitude increases, intake temperature decreases, and so burner inlet temperature. As a result, expansion in the turbine is higher, and so jet exhaust speed  $V_9$ . According to eq. 2.54, specific thrust increases. Note that an increment in  $V_{19}$  is also got, but this contribution turns negligible due to the very low value of by-pass ratio (see table 4.1). Besides, higher thrust leads to higher fuel consumption, as observed in fig. 4.8 (left).

The effect of mach number is the opposite: the higher the mach, the lower the thrust and hence the consumption. The reason is the following: airspeed increases air inlet temperature, just like a decrease in altitude. Thereby, the effect is analogue to the one explained above.

On the other hand, engine weight is only affected by Mach number. The reason behind this is that, according to Torenbeek's formula, weight-to-thrust ratio depends on pressure and bypass ratio, which do not depend on neither of the variables. There is also a dependence on sea-level specific thrust, whose value does not vary with altitude, obviously. Increasing Mach means less thrust, and so more weight.

Note that there is a zone where no solution is found: if both speed and altitude are very low, inlet temperature increases in such a way that after compression higher temperature than fixed  $T_{4t}$  is got. This may suppose a problem for takeoff phase, however, this study has been conducted assuming cruise conditions, so a different configuration from the one shown in sec. 4.2 may be selected.

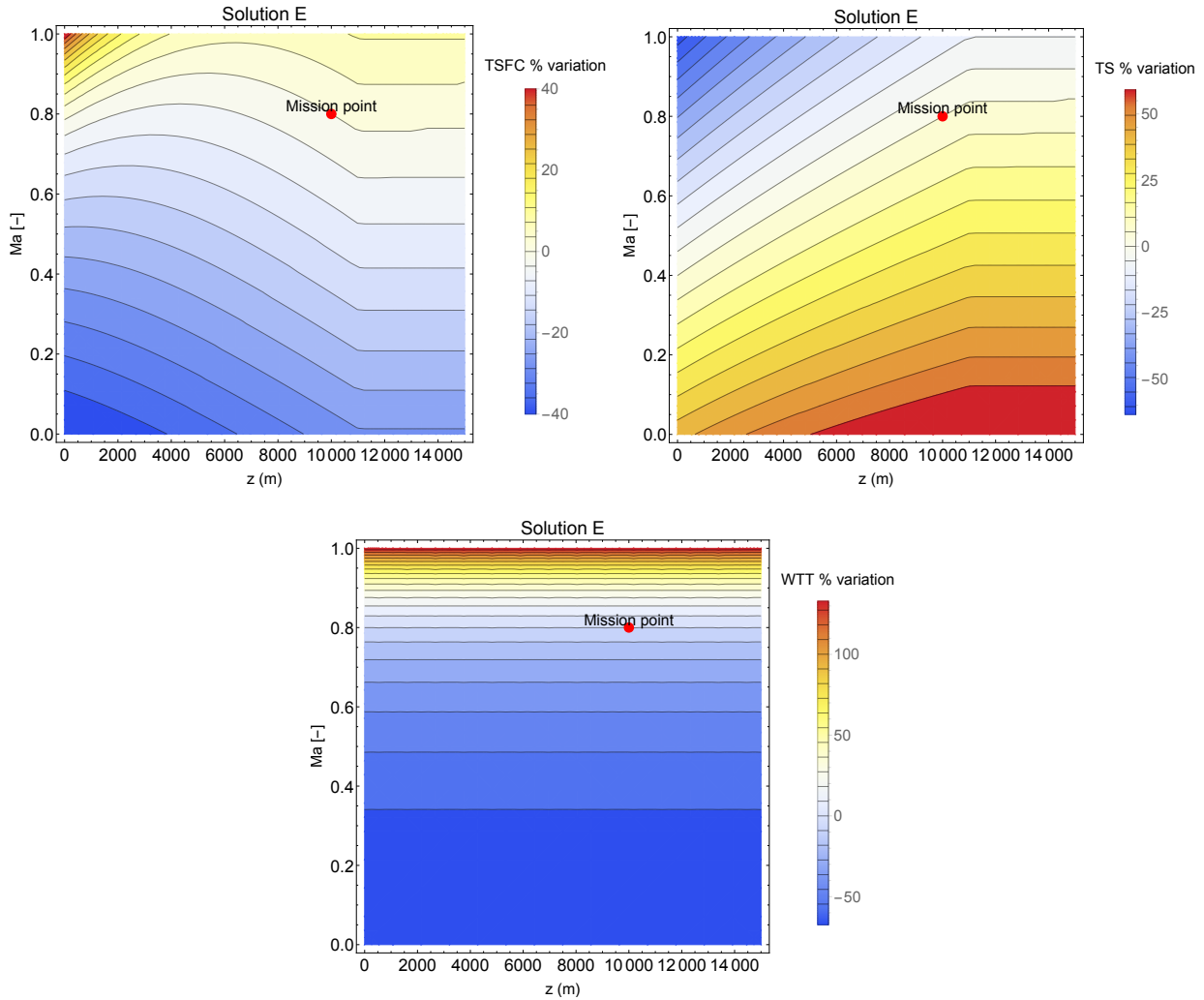


Figure 4.9: From left to right and top to bottom: engine performance variation as a function of mission parameters for configuration solution E.

Results for optimum point E are presented in fig. 4.9. Results can be approached to the ones shown for the previous solution point. However, a difference in specific fuel consumption is found: the effect of altitude cannot be generalised.

The reason behind this behaviour relies in eq. 2.57: according with the previous analysis, an increasing altitude leads to an increasing fuel consumption provided that specific thrust increases. However, the influence of fuel-air ratio has not been considered: if altitude increases, this parameter too, so a fight among both numerator and denominator is found. Depending on the flight regime, one dominates the other. Hence, there is a particular value of altitude where consumption has a minimum, for a given mach number.

It is also noted that no unsolvable regions are found in this particular case. Given the design conditions presented in table 4.1, a high pressure ratio decreases the system failure probability.

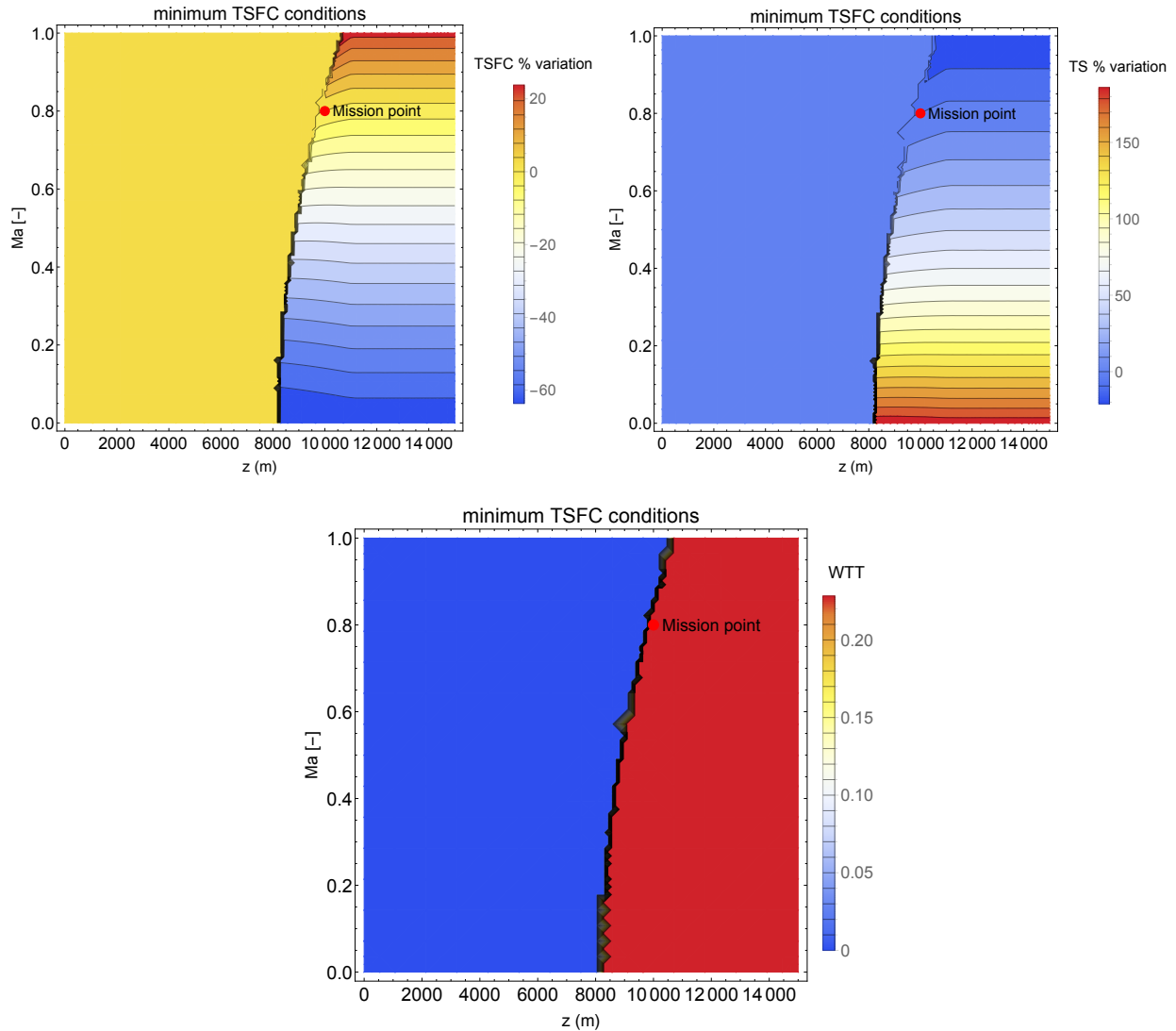


Figure 4.10: From left to right and top to bottom: engine performance variation as a function of mission parameters.

Observing fig. 4.10, left, an increase in fuel consumption is observed for higher mach numbers. The explanation is the following: a direct impact on speed velocity,  $V_0$ , is got. Then, since compression stage starts at a higher stagnation temperature, combustion temperature is reached at a higher pression, so a higher jet speed is given. Moreover, a little increment in  $V_9$  also happens, because of isobars divergence. So, analysing eq. 2.54, no clear trend can be established. Nonetheless, since increment in flight speed is quite higher than jet one,  $V_0$  dominates in the equation, resulting in a thrust reduction. Fuel consumption, on its hand, increases with mach number, since it has an inverse relation with specific thrust, as eq. 2.71 states.

The influence of the altitude, however, is less pronounced. When decreasing in altitude, farfield temperatures are greater. Therefore, the cycle starts at a higher point. If TIT is fixed, this means a smoother combustion, so fuel-to-air ratio decreases. The same happens to exhaust velocity in the nozzle, since air pressure is higher and combustion one remains constant. The secondary nozzle, however, experiments a small increase: since isobars tend to diverge, the same pressure step means greater steps in temperature -and hence in velocity- is, no more modifications (i.e. combustion) are

given.

So, given eq. 2.54, no trends in specific consumption can be stated, since individual trends are confronted. Thus, the behaviour may be unexpected. In fact, for low mach numbers, secondary nozzle jet speed dominates, and thrust decreases with altitude. On the other hand, when flight speed is higher, primary flow becomes more important, and the opposite trend is got.

Note that, when changing altitude, both thermal and pressure conditions change. However, only the former seems to affect results, since no changes in results are observed when changing altitude conditions after the tropopause.

Regarding fuel consumption, it can be set that a dependance on both fuel ratio and thrust is given, according to eq. 2.71. It can be proved that fuel injected does not suffer greater changes whatever external conditions are, although a trend exists [4]. Then, fuel consumption is dominated by specific thrust, having opposite behaviours. For this reason, a TSFC increment can be stated for lower values of TS, and viceversa. Also, more pronounced variations can be observed in thrust, compared to fuel consumption. Hence, changes in mission will mainly affect this performance parameter.

Regarding engine weight, a constant value is given for the whole domain. This is because of the correlation used to calculate weight: being characterised the minimum TSFC point by a high BPR, Jenkinson's formula (eq. 2.74) is used. Only BPR dependance is stated in these conditions, so neither flight velocity nor altitude change this parameter.

Finally, it can be observed that the mission point is very close to the limit of solvability. According to fig. 4.10, if altitude is reduced or speed is increased, the cycle cannot stand this situation, so some conditions in the design point are not the same any more. This behaviour, although not critical, is important to know, since engine will adapt itself to the conditions established.

Next, in fig. 4.11, the same analysis has been conducted for different design conditions. In this case, thrust maximization is aimed, so a very low bypass ratio is got. The rest of the parameters in the design, however, do not experiment considerable changes.

First, the influence of mach is analysed: as happened in the previous study, fuel consumption increases when mach is increased, as well a decrease in engine thrust is observed. The behaviour under this trend is similar to the one explained before: airspeed increases significantly, and, although exhaust velocity also does, the former is more pronounced, so a reduction in thrust is got.

The dependance on altitude, however, is not the same. In this case, a uniform trend can be observed for the whole domain. The trends in the cycle are the same, provided that a change in secondary flow does not affect this part. Nonetheless, attending to eq. 2.54, a dependance on  $\beta$  is observed. Hence, since this parameter is close to zero, it can be neglected, and thrust can be just simplified to the diminish among jet and aircraft velocities. On it,  $V_9$  is the dominant, and specific thrust grows.

This trend can be considered as a permanent domination of the primary nozzle, since secondary massflow is very low. In the previous case, bypass ratio strengthened the effect of  $V_{19}$ , whose changes were not very pronounced. The product, however, was not negligible, and general trend facing was given, even changing the direction in some cases. Here, no facing is got, so trends are more pronounced and always in the same direction.



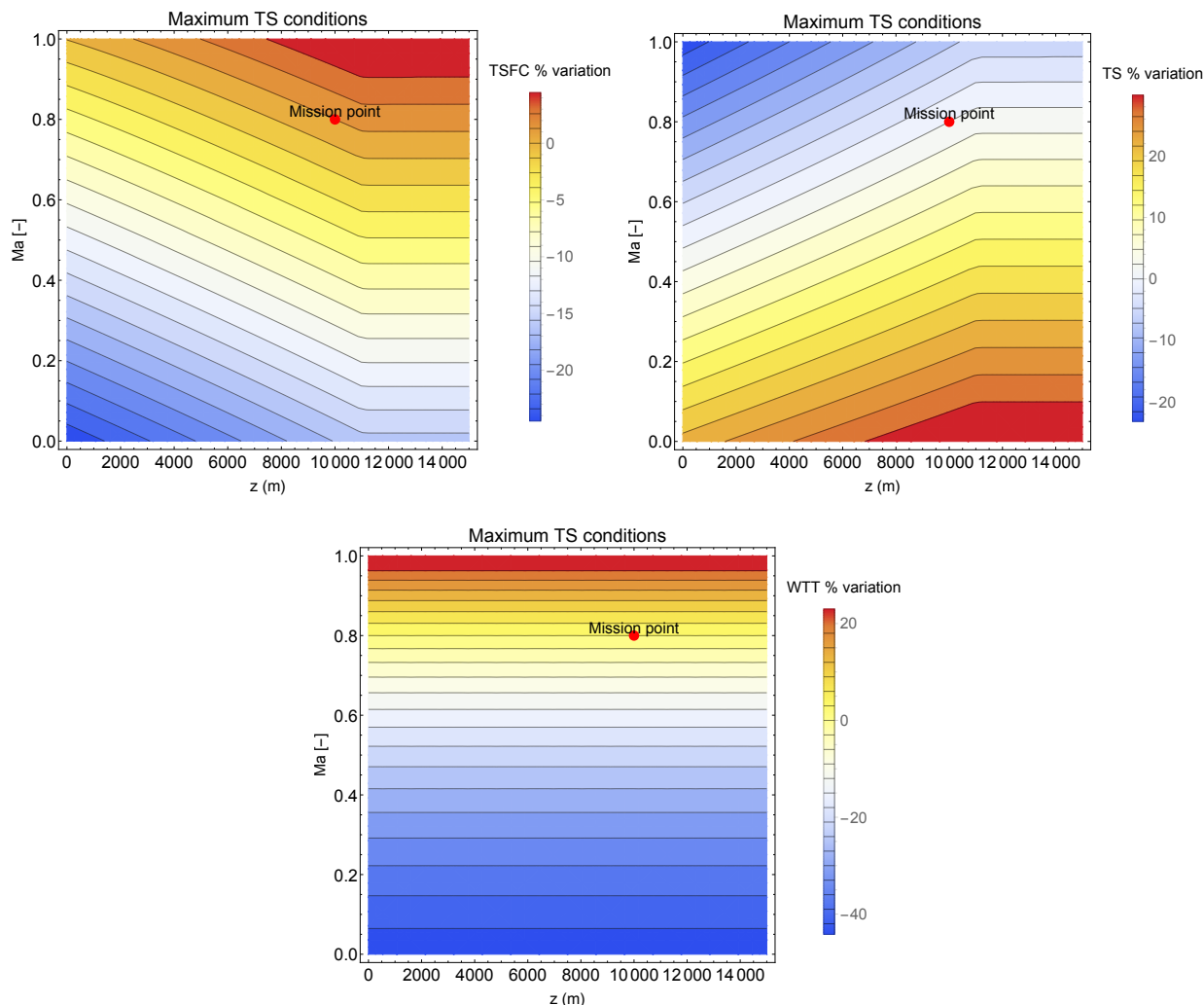


Figure 4.11: From left to right and top to bottom: engine performance variation as a function of mission parameters.

Again, ambient pressure is not relevant in the study.

Weight changes can be observed in fig. 4.11, down. Note that percentual variations in the domain are less pronounced than in the previous point. That means this selection is more stable than the other. In this case, since BPR is very low, Torenbeek's approach (eq. 2.73) is used. It can be observed that all magnitudes appearing in it remain constant whichever the mach, except take-off specific thrust. This variable is simply a particular case of thrust, fixing  $z = 0$ . So, observing fig. 4.11, right, a decrease in thrust when mach rises is given, and thereby weight-to-thrust ratio increases.

Finally, no unsolvable regions are found, unlike the previous design point. Here, conditions are less restrictive: turbine inlet temperature is greater, while compression is lower. These trends tend to increase the range on which solutions can be performed.

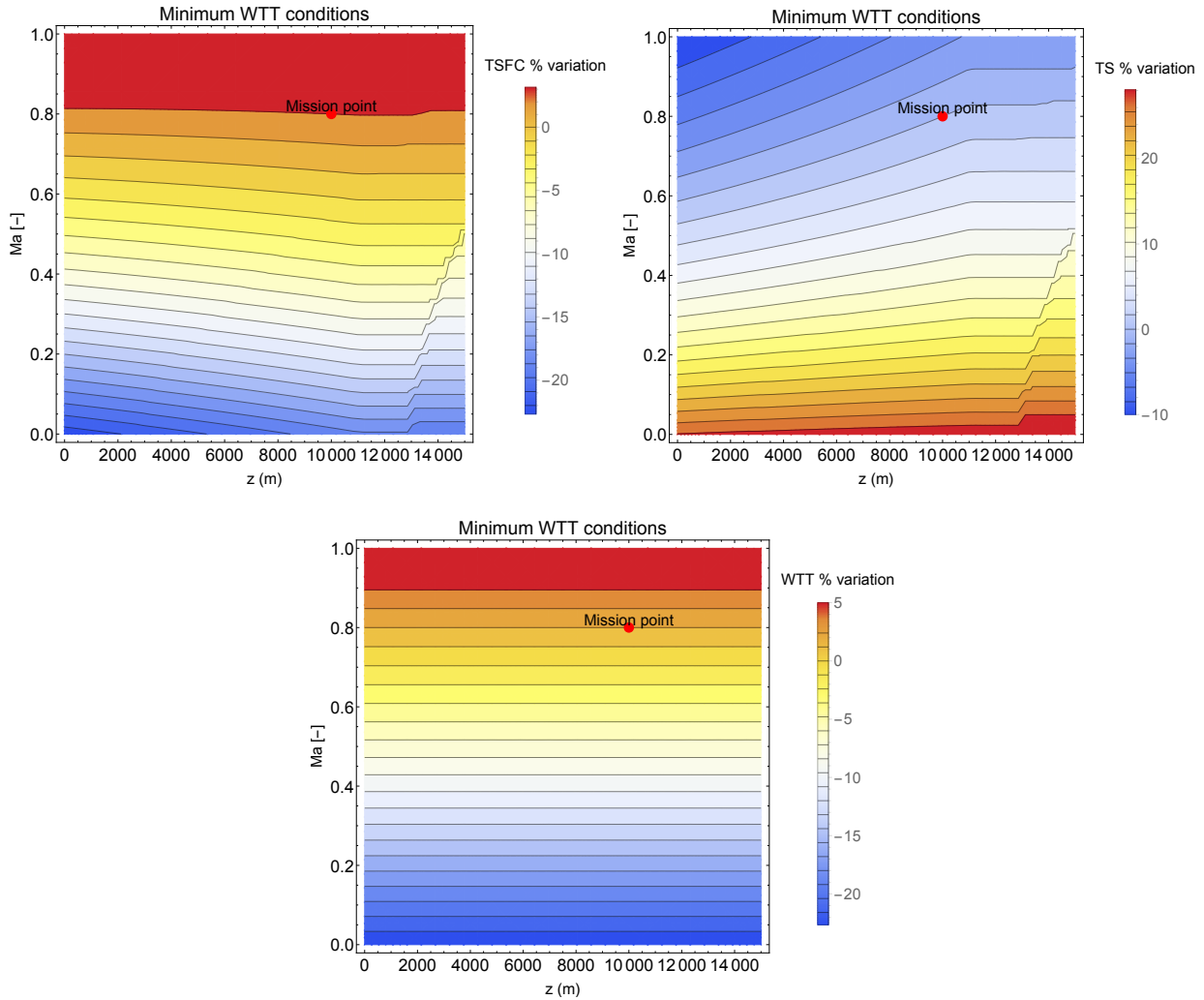


Figure 4.12: Example of a sensitivity chart.

Finally, in fig. 4.12, the lightest configuration has been selected. On it, compression makes a total of less stages, since the more stages the heavier the structure is. Moreover, bypass ratio is also low, to avoid a big fan. The compression in the fan is slightly greater than in the compressor.

Again, when increasing mach number, specific thrust is reduced and fuel consumption increases. Nonetheless, the change is harder for low speed conditions. After that, velocity difference among surrounding air and exhaust becomes lower, but still dominated by  $V_0$ , so a smoother gradient is observed.

The influence of the altitude is in this case lower. This fact is due to the low compression performed in the cycle: provided that difference in velocities are motivated by isobars divergence, if pressure during combustion is closer to the atmospheric one, less divergence is got, and hence less changes in speed are given. Nonetheless, the phenomena under the plots are the same, and so the trends. Note that an increase in mach allows higher influence: when speed is applied to the fluid, combustion occurs at a higher pressure, and more difference  $V_9 - V_0$  is got.

Finally, weight behaviour is similar to the one observed for best thrust conditions: correlation applied is the same, and the gradient follows the shape of specific thrust plot.

### 4.3.2 Component efficiencies

Finally, the same study is performed for the engine components: its efficiency is changed and performance parameters are presented as a function of the individual variation of each component.

First, the three variable tradeoff is presented. Relative deviations in all performances are plotted as a function of each component efficiency. The zero-crossing shows the nominal value used.

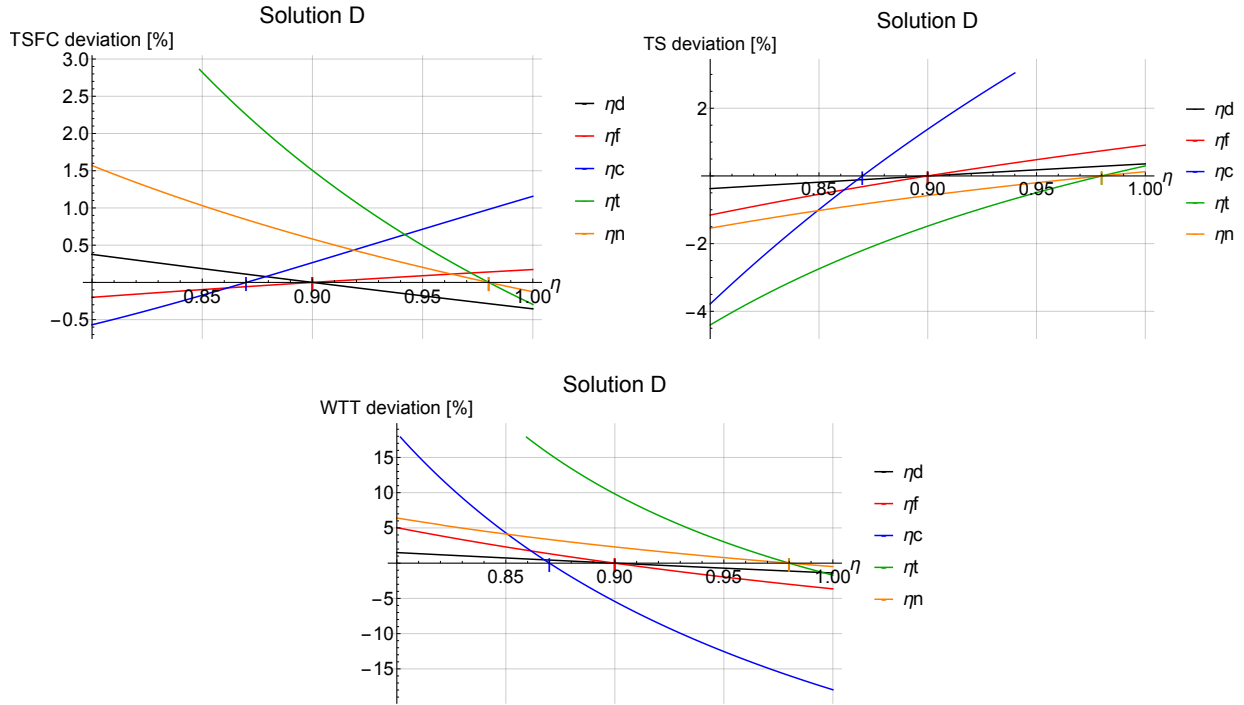


Figure 4.13: From left to right and top to bottom: engine performance variation as a function of engine components isentropic efficiency for case solution D.

According to fig. 4.13, engine turbine seems to be the most critical component. Provided that the biggest pressure ratio is carried out in this component, higher variations are found. The nozzle is also giving not negligible steps, particularly regarding to fuel consumption. The fact behind this trend is that jet speed at exhaust,  $V_9$ , is hardly varying during the expansion stage.

Few compressing components, such as difusor and fan, have a low incidence, since, if low compression is performed, so will be the variations in speed available.

A particular behaviour is observed for the compressor: more efficient compressors lead to an increase in fuel consumption. The reason relies on the fuel-to-air ratio: if a more efficient compressor is set, the parameter  $T_{3t}$  decreases, so  $f$  increases, according to eq. 2.22. This fact leads to an increase of  $V_9$  which rises specific thrust, as observed in fig. 4.13, right. Since both trends are faced to each other in the case of consumption, a dominance of  $f$  can be stated.

Finally, weight-thrust ratio follows the same trend as fuel consumption, without the exception of the compressor. In fact, its behaviour is just the opposite from thrust, according to Torenbeek's correlation. Moreover, this is the most sensitive parameter, since variations until 15% can be reached.

Next, the same results are presented in fig. 4.14 for the solution proposed named as E.

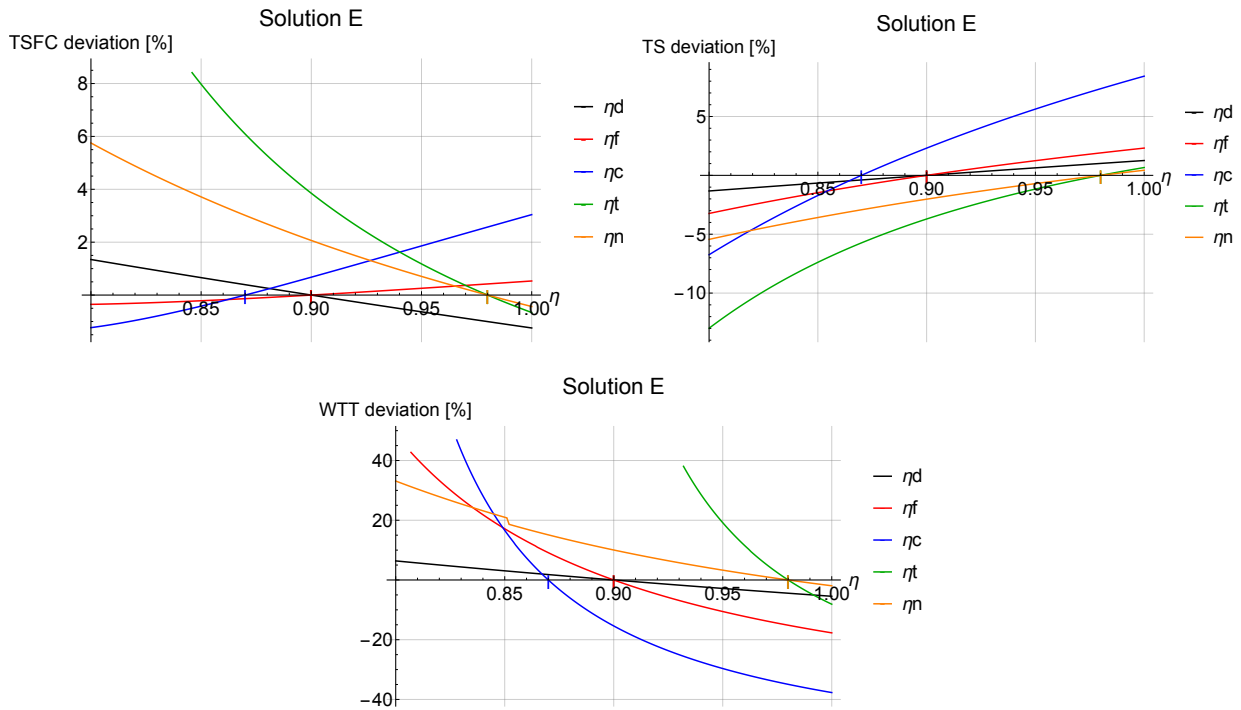


Figure 4.14: From left to right and top to bottom: engine performance variation as a function of engine components isentropic efficiency for case solution E.

The same trends are observed for this case. The difference relies on the nominal values appearing: this configuration is more sensitive to changes, given the higher pressure ratio applied that increases the scale of the Brayton cycle, leading to higher steps both in compression and expansion. Hence, variations in jet exhaust speed may be higher.

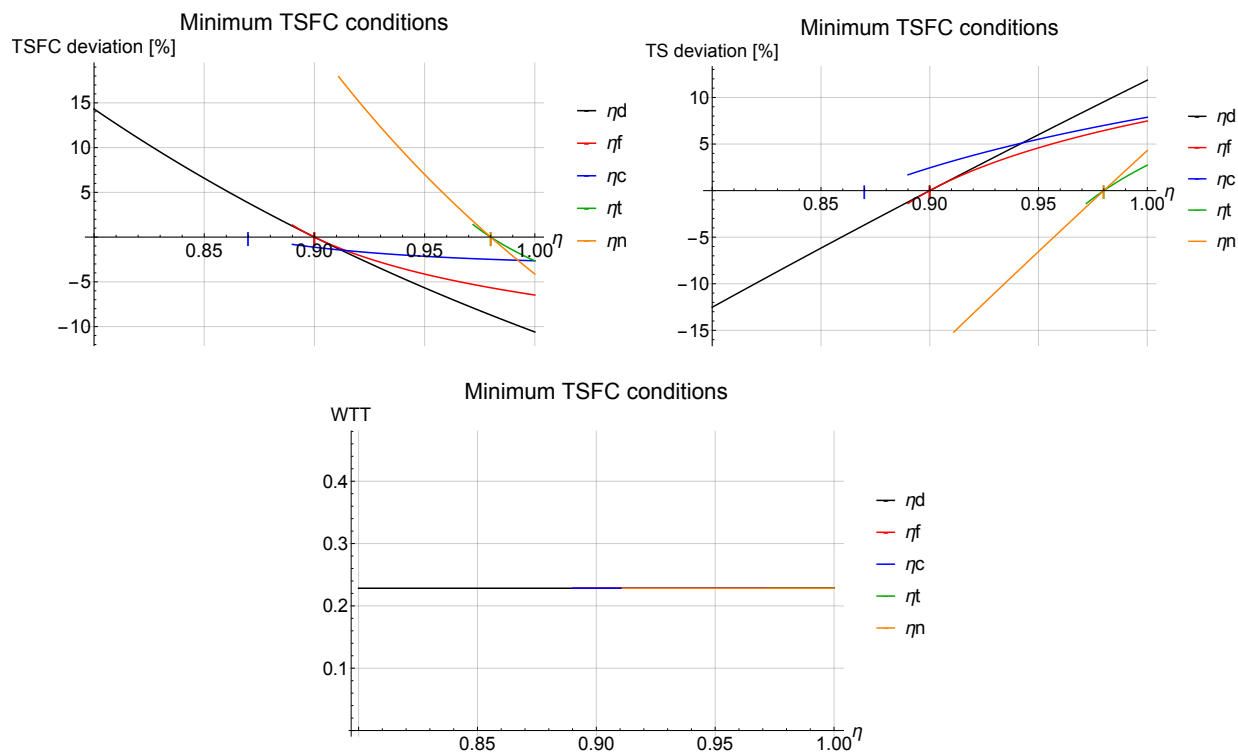


Figure 4.15: From left to right and top to bottom: engine performance variation as a function of engine components isentropic efficiency.

Observing fig. 4.15, performance improves when components are more efficient, as supposed. First, the influence of diffusion is analysed: if the intake process is more efficient, point  $2t$  gets closer to  $0t$ . In the perfect case, both stations coincide. If the rest of the components are not modified, this improvement in the intake means higher pressures in both fan and compressor. Combustion process is not modified, provided that working temperatures remain unchanged. This pressure delta is moved along the whole cycle, until the nozzle, where more flow expansion is performed. As a result, jet exhaust velocity increases. The same analysis is applicable to the second nozzle, so  $V_{19}$  also increases.

By observing eq. 2.54, and considering that aircraft speed is not changing, an increase in specific thrust is given. It is important to remark that both jet increases are small. However, since minimum TSFC conditions require high bypass ratio, the contribution of secondary jet exhaust becomes not negligible, according to eq. 2.54. As a result, TS gains up to 10% can be obtained.

Fuel consumption follows the opposite trend: according to eq. 2.56, an increase in specific thrust leads to a decrease in fuel consumption.

Note that the intake process is one of the most sensitive to changes, provided that this is the first component of the cycle and eventual changes in this part may be swept -and even amplified- along the cycle.

Both compressor and fan follow the same explaining: when a more efficient compression is held, the enthalpy step on it is lower. In other words, the same compression requires less work in a more efficient component. As a result, turbine will use less work to move the compressor, resulting on an increase in stage  $5t$ . Again, pressure step in the nozzle becomes higher, and so  $V_9$  -and  $V_{19}$  in the case of fan efficiency increase. So, specific thrust increases, and fuel consumption decreases, according to eqs. 2.54 and 2.57, respectively.

Note that fan can generate better improvements in the performance, although pressure changes

in this component are quite lower than the ones found in the compressor. Again, by-pass ratio becomes fundamental, giving a greater importance to the secondary flow.

Core turbine, on its hand, performs lower expansion when working in more efficient conditions: since the enthalpic step -and then thermal- is fixed by the compressor, if entropy increase is lower, turbine exit  $41t$  will be placed to the left, but at the same temperature. Again, expansion held in the nozzle is greater, and so exhaust velocity. As a consequence, thrust increases as well as a reduction in fuel consumption is got. Note that gains under turbine improvements are not very high, since the efficiency of this component is commonly high on itself.

Regarding nozzles, the following process happens: in a more efficient nozzle, temperature step on it is higher, and so jet speed. The result is the same than other shown before. Note that this is the most sensitive component, provided that it is the one where the highest pressure step occurs. Moreover, the contribution of bypass ratio makes the difference in thrust higher.

Note that the cycle cannot stand low efficiencies of most of components. This is due to the low margin to unstable conditions best consumption conditions have, as shown in fig. 4.10. This is one more reason for the development of more efficient components.

Finally, no changes in weight-to-thrust ratio are observed. Since this parameter depends only on bypass ratio under these conditions, and this variable is external to the cycle, a constant value is got for the whole study.

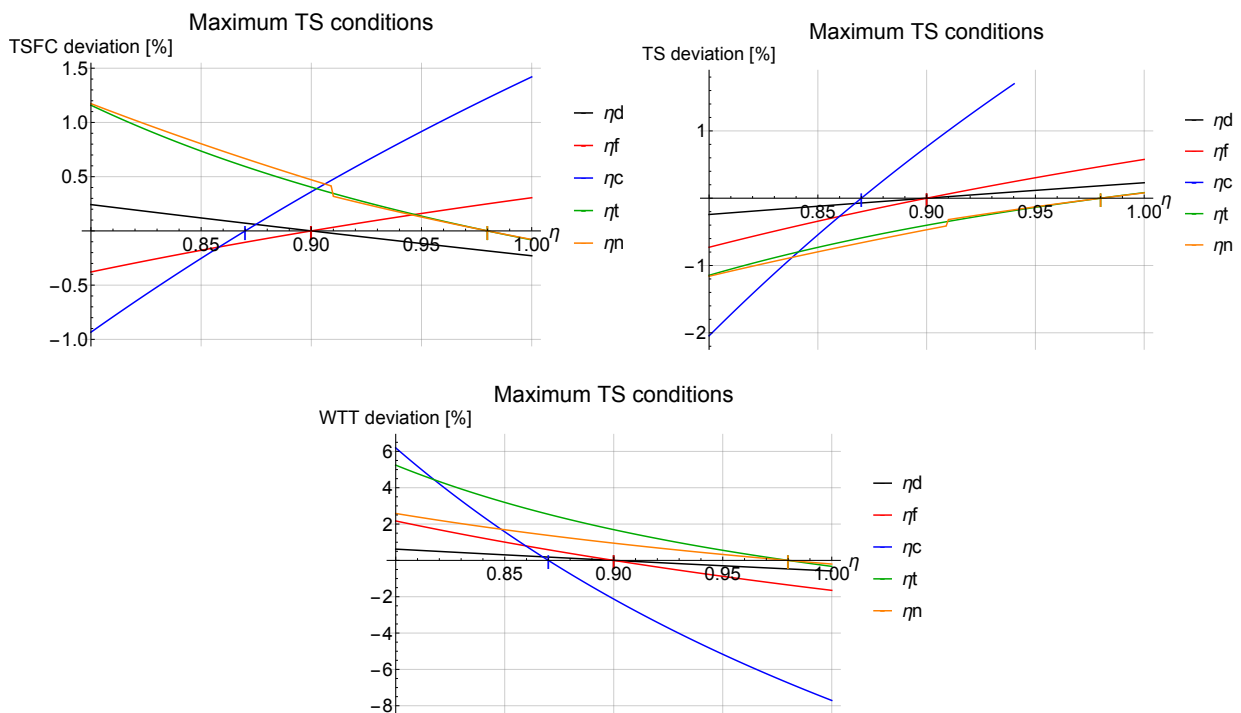


Figure 4.16: From left to right and top to bottom: engine performance variation as a function of engine components isentropic efficiency.

In fig. 4.16, an analogue study is conducted, assuming maximum specific thrust. In this case, BPR is very low, and, as a consequence, changes in secondary flow exhaust speed can be considered negligible. Hence,  $V_9$  becomes the only parameter to be analysed.

Diffusion process follows the same behaviour: pressure is grown resulting as a last resort on a faster jet. This contributes to a better specific thrust. However, since the effect of the secondary jet is very low, no pronounced improvements can be reached.

The same reasoning can be applied to the rest of components. Since higher expansions take place in high pressure turbine and nozzle, these perform the highest changes in the performance.

A particular behaviour is observed for both fan and compressor: an opposite trend is got for the specific fuel consumption, which is unintuitive at a first thought. The reason is in its exit temperature, that is, parameter  $T_{3t}$ ; in a more efficient compressor, temperature is reduced and, according with eq. 2.17, fuel-to-air ratio increases. Studying eq. 2.57, and considering that specific thrust is higher as a result of  $V_9$  improvement, no clear tendence can be explained. However, the growth in  $f$  is higher than the one found in TS, provided that bypass ratio is very low and hence specific thrust does not increase too much. This is the only case in which  $f$  dominates, due to very particular conditions: a big compression held -as happens in the main compressor- and low bypass ratio, that leads to low variations of specific thrust.

Finally, the analysis of weight is analysed: attending to eq. 2.73, weight-to-thrust ratio is directly linked to specific thrust. If the latter increases, the former decreases, and viceversa.

Note that compression system is the most sensitive component, since the highest pressure steps are held on it. Nonetheless, improvements available are less than in the previous conditions, since secondary flow is limited and hence modifications are not amplified because of it. An exception occurs to weight, where improvements until 8% can be achieved.

In this case all domain study seems to be solvable, due to less restrictive conditions in best thrust point.

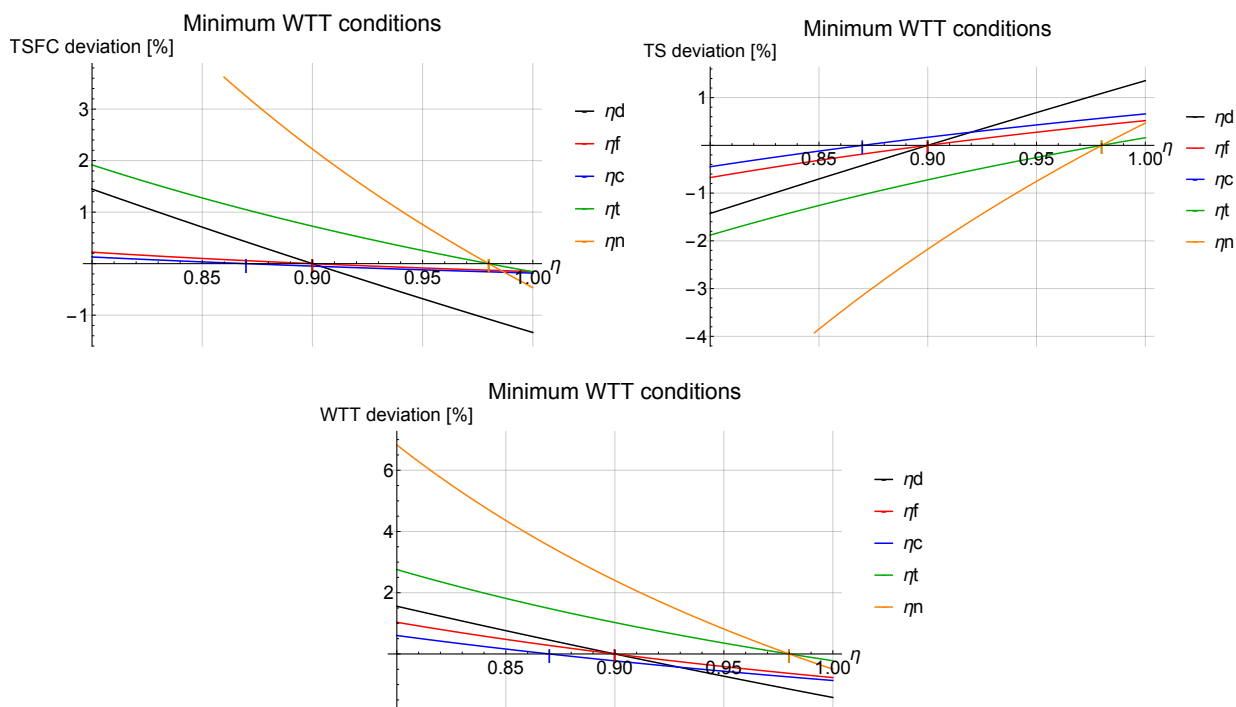


Figure 4.17: From left to right and top to bottom: engine performance variation as a function of engine components isentropic efficiency.

Finally, minimum weight-thrust ratio conditions are studied. In fig. 4.17, variations in engine performance when modifying component efficiencies can be observed. This working point is characterised by a very low pressure ratio in the compressor and a higher one in the fan. The overall step, however, is quite lower.

The same trends can be assumed, however, a decrease in compressor's influence can be reported.

The reason is that, since jet speed variations -which in the end controls all performances- are motivated by high pressure steps, if low compression is given the influence of this component becomes quite less. Nonetheless, the trend is the same than the ones for the other parts, unlike best thrust point: lower compression leads to small changes in  $T_{3t}$ , and hence in the compressor, as well as a little bit higher bypass ratio helps in the dominance of TS opposite  $f$ .

On the other hand, weight follows the same approach performed for the previous study: an inverse dependance of weight with thrust is observed.



## Chapter 5

# Discussion of results

A brief discussion is now performed in order to clarify optimums found and potentially selected. The reduction of engine specific fuel consumption is faced to specific thrust requirements. A proper selection may consider good properties of both parameters, as well as a reasonable value for weight-thrust ratio, which follows the opposite evolution than the previous variables mentioned. Taking local optimums may not be a good practice, since dramatic harm in the rest of the parameters studied has been proved.

On the Pareto front, a family of aircraft is modeled: from very tiny aircraft to most powerful fighters, passing through commercial aviation. The mission requirements stated set the zone to be selected in the front. Regarding airlines, field to which this project has been oriented, focus on fuel consumption should be performed, ensuring that aircraft demands are fulfilled in terms of thrust and lift/drag. Provided that low consumption engines are heavier, an economical study involving spends and benefits in both issues should be carried out.

On the other hand, turbofan bypass ratio has been postulated as the controlling parameter in performance. When flow bypassed is higher, secondary flow becomes more important, and improvements in the overall performance can be reached. Engine core, although more complex, cannot perform such huge changes.

When studying off-design conditions, but still steady, differences in engine performance are observed. Concerning mission parameters, flight speed and altitude may change both thrust and consumption. Variations that lead to a farfield energy increment tend to reduce fuel consumption, whereas bank conditions may increment specific thrust. Weight is also modified if bypass ratio is low enough, according to correlations used in this project.

Engine components also play an important role in engine performance. The greater the pressure ratio in the component itself is, the higher variations may be reached. In the end, an increase of jet exhaust speed is searched to increase specific thrust, as well as low fuel-air ratio that allows consumption decrease. More efficient components perform better results, with the particular exception of compressor in some cases. In them,  $f$  dominates exhaust conditions, facing the common -and intuitive- trends.

Results concerning performance variations are obtained considering fixed design parameters only. In other words, mission parameters and component isentropic efficiencies have not been included in the optimum, but studied a posteriori. Thereby, local optimums have been studied only, and wider analysis has to be conducted to obtain a whole engine optimization for the mission requirements stated.



## Chapter 6

# Conclusions and future works

Next, main conclusions obtained after conducting this project are presented, as well as future studies that may be carried out as a continuation of this one.

### 6.1 Conclusions

Once the project has been finished, it can be stated that objectives set at the beginning of this document have been accomplished, being established the following conclusions:

- A Pareto front concerning fuel consumption and specific thrust has been obtained. Moreover, the variable concerning engine weight has been included satisfactorily. A relation in the optimum search behaviour between weight and thrust has been found.
- Bypass ratio has been stated as the dominant design parameter in the results. Particularly, remarkable fuel consumption decrease has been connected to high BPR. Hence, the use of turbofan engines with increasingly bigger fans in commercial aviation has been justified, as long as the objective of companies is to reduce spendings as much as possible.
- Exhaust jet speed and fuel-air ratio can model both specific thrust and consumption, respectively. Their trends are usually faced to each other, however, a dominance of jet speed in the nozzle has been proved in most of cases, which confirms the behaviour stated in bibliography.
- All trends observed for both optimums and sensitivity analysis are in accordance with the ones stated by the authors. Hence, the model used to calculate engine performance, based on a simplified the Brayton cycle, has been validated.

### 6.2 Future works

After concluding this work, several projects that might be a continuation of this one can be stated:

- On the one hand, engine dimensioning can be carried out after knowing thrust required by the aircraft. In this way, mass flow can be fixed and the detail design of all components, particularly compressor and fan, may be performed.
- Next, the inclusion of both design and performance parameters could be interesting: component efficiencies could be included in the optimum research, as well as cycle efficiencies presented in the theoretical background can be considered as parameters that are also important to optimise. Nonetheless, a factorial increase in the computational effort required to carry out this study should be considered.

- Finally, engine behaviour study under off-design conditions, such as takeoff and landing, is planned.

# Bibliography

- [1] Several Authors. Turbofan engine. *Journal*, 2017.
- [2] Several Authors. Propulsión: Clasificación de sistemas propulsivos. *Universitat Politècnica de València - Departamento de Máquinas y Motores Térmicos*, pages 19;24–25;49;51, 2016.
- [3] Mauro Valorani and Riccardo M. Galassi. Motori aeronautici: Control volume analysis. *Sapienza Università di Roma*, 2019.
- [4] Several Authors. Ampliación de aerorreactores y aeroacústica: Optimización de motores turbohélice. *Universitat Politècnica de València - Departamento de Máquinas y Motores Térmicos*, page 5, 2017.
- [5] Several Authors. Ampliación de motores alternativos: Introducción a los mcia. *Universitat Politècnica de València - Departamento de Máquinas y Motores Térmicos*, page 7, 2017.
- [6] Mauro Valorani and Riccardo M. Galassi. Motori aeronautici: il ciclo brayton. *Sapienza Università di Roma*, 2019.
- [7] Several Authors. Propulsión: Generación de empuje y prestaciones. *Universitat Politècnica de València - Departamento de Máquinas y Motores Térmicos*, page 25;46, 2016.
- [8] E. Torenbeek. Synthesis of subsonic airplane design. *Martinus Nijhoff*, pages 129–130, 1975.
- [9] P. E. Lolis. Evaluation of aero gas turbine preliminary weight estimation methods. *The Aeronautical journal*, 118:4, 2014.
- [10] L.R. Jenkinson, P. Simpkin, and D. Rhodes. Civil jet aircraft design. *Butterworth-Heinemann*, pages 139–140, 1999.
- [11] Mustafa Cavcar. The international standard atmosphere (isa). *Anadolu university*, page 4.
- [12] Enrico Rigoni and Silvia Poles. Nbi and moga-ii, two complementary algorithms for multi-objective optimizations. *ESTECO S.r.l*, page 3.
- [13] Several Authors. Multi-objective generic algorithm (moga). 2019.
- [14] Jeffries W. Chapman, Thomas M. Lavelle, Ryan M. May, Jonathan S. Litt, and Ten-Huei Guo. Toolbox for the modeling and anlysis of thermodynamic systems (t-mats). *NASA's newsletter*, 2014.
- [15] Mark H. Waters and Edward T Schairer. Analysis of turbofan propulsion system weight and dimensions. *NASA Technical Memorandum*, 1977.
- [16] Aaron R. Byerley, August J. Rolling, and Kenneth W. Van Teruen. Estimating gas turbine engine weight, costs, and development time during the preliminary aircraft engine design process. *Turbine Technical Conference and Exposition*, 2013.